

# 1 **Spatial and temporal oxygen isotope variability in northern** 2 **Greenland – implications for a new climate record over the** 3 **past millennium**

4  
5 **S. Weißbach<sup>1</sup>, A. Wegner<sup>1</sup>, T. Opel<sup>2</sup>, H. Oerter<sup>1</sup>, B. M. Vinther<sup>3</sup> and S. Kipfstuhl<sup>1</sup>**

6 [1]{Alfred Wegener Institut Helmholtz-Zentrum für Polar- und Meeresforschung,  
7 Bremerhaven, Germany}

8 [2]{Alfred Wegener Institut Helmholtz-Zentrum für Polar- und Meeresforschung, Potsdam,  
9 Germany}

10 [3]{Centre for Ice and Climate, Niels Bohr Institute, University of Copenhagen, Denmark}

11 Correspondence to: S. Weißbach ([stefanie.weissbach@awi.de](mailto:stefanie.weissbach@awi.de))

12

## 13 **Abstract**

14 We present for the first time all 12  $\delta^{18}\text{O}$  records obtained from ice cores drilled in the framework  
15 of the North Greenland Traverse (NGT) between 1993 and 1995 in northern Greenland. The  
16 cores cover an area of 680 x 317 km, 10 % of the Greenland ice sheet. Depending on core length  
17 (100-175 m) and accumulation rate (90-200 kg m<sup>-2</sup> a<sup>-1</sup>) the single records reflect an isotope-  
18 temperature history over the last 500-1100 years.

19 Lowest  $\delta^{18}\text{O}$  mean values occur north of summit and east of the main divide as a consequence  
20 of Greenland's topography. In general, ice cores drilled on the main ice divide show different  
21 results than those drilled east of the main ice divide that might be influenced by secondary  
22 regional moisture sources.

23 A stack of all NGT records and the NGRIP record is presented with improved signal-to-noise  
24 ratio. Compared to single records, this stack represents the mean  $\delta^{18}\text{O}$  signal for northern  
25 Greenland that is interpreted as proxy for temperature. Our northern Greenland  $\delta^{18}\text{O}$  stack  
26 indicates distinctly enriched  $\delta^{18}\text{O}$  values during medieval times, about 1420±20 AD and from  
27 1870 AD onwards. The period between 1420 AD and 1850 AD has depleted  $\delta^{18}\text{O}$  values  
28 compared to the average for the entire millennium and represents the Little Ice Age. The  $\delta^{18}\text{O}$   
29 values of the 20<sup>th</sup> century are comparable to the medieval period but are lower than that about  
30 1420 AD.

## 1 **1 Introduction**

2 During the past decades the Arctic has experienced a pronounced warming exceeding that of  
3 other regions (e.g. Masson-Delmotte et al., 2015). To set this warming into an historical context,  
4 a profound understanding of natural variability of past Arctic climate is essential. To do so,  
5 studying climate records is the first step. However, meteorological measurements in the Arctic  
6 are only available for relatively short time periods; only a few time series start already in the  
7 19<sup>th</sup> century. Hence, proxy data from climate archives such as ice cores from the polar ice caps  
8 are essential.

9 Studying the climate of the past centuries allows us to compare the instrumental data with proxy  
10 records and therefore to assess the quality of the proxies for climate reconstructions.

11 Stable water isotopes (here  $\delta^{18}\text{O}$ ) in ice cores are commonly used to derive paleo-temperatures  
12 (e.g. Fischer et al., 1998c; Johnsen et al., 2000; Steffensen et al., 2008). They are largely  
13 controlled by equilibrium and kinetic fractionation processes during evaporation at the ocean  
14 surface, along the poleward air-mass transport and condensation of precipitation, depending on  
15 temperature and moisture conditions (Dansgaard et al., 1969; Jouzel and Merlivat, 1984;  
16 Merlivat and Jouzel, 1979).

17 The isotope ratio is not only driven by local temperature, but is affected by several factors like  
18 moisture sources and their proximity to the deposition site, the topography of the ice sheet and  
19 the seasonality of precipitation (Fisher et al., 1985). In addition the isotope signal is altered by  
20 post-depositional processes like wind-induced redistribution of snow, temperature gradient  
21 metamorphism and diffusion (Johnsen et al., 2000; Pinzer et al., 2012; Steen-Larsen et al.,  
22 2014). Stacked records are used to compensate for effects due to local to regional differences  
23 and to improve the signal-to-noise ratio (Fisher et al., 1985; Masson-Delmotte et al., 2015;  
24 White et al., 1997).

25 To date, most ice core studies on the Greenland ice sheet were carried out point wise (e. g. Dye  
26 3, GRIP, GISP2, NGRIP), which poses the question: How representative is one single long ice  
27 core record to derive a comprehensive record of past climate? A study of ice cores from  
28 southern Greenland revealed that winter season stable water isotopes are largely influenced by  
29 the North Atlantic Oscillation (NAO) and are strongly related to southwest Greenland air  
30 temperatures. On the other hand, summer season stable water isotope ratios show higher  
31 correlations with North Atlantic sea surface temperature conditions (Vinther et al., 2010). In  
32 particular, northern Greenland has been little investigated so far. The summit in Greenland's  
33 center is the highest site and separates Greenland in a northern and southern part. Northern

1 Greenland differs significantly from the south in terms of lower air temperatures and lower  
2 snow accumulation rates (Fischer et al., 1998c). Thus, the results from southern Greenland are  
3 not directly transferable to the northern part.

4 Northern Greenland's climate is influenced by different effects than the southern part. One  
5 example is the NAO effect which is present in southern and western part of Greenland and is  
6 discussed to be reduced in northern Greenland (Appenzeller et al., 1998).

7 The cyclones causing the precipitation over northern Greenland originate in the Baffin Bay and  
8 bring dry and cold air masses from the central Arctic to north Greenland (Chen et al., 1997).

9 The dominant westerly winds are blocked by the ice divide while the north eastern part has very  
10 low accumulation rates below  $100 \text{ kg m}^{-1} \text{ a}^{-1}$ .

11 The topographic situation in northern Greenland is special for  $\delta^{18}\text{O}$  studies. In northern  
12 Greenland going northward also means to go downward (lower altitudes).

13 For a correct estimate of mass balances as well as the response to the ongoing climate change,  
14 knowledge of accumulation rates and the spatial distribution of  $\delta^{18}\text{O}$  as a temperature proxy are  
15 important for the entire Greenland ice sheet. However, due to northern Greenland's remoteness  
16 its recent past climate has, up to now, only been little investigated.

17 Even in the 1990s little was known about northern Greenland. Only few studies were performed  
18 before Alfred-Wegener Institute (AWI) North-Greenland-Traversal (NGT) started in 1993.  
19 There was a traverse of Koch and Wegener in 1913 (Koch and Wegener, 1930), of Benson in  
20 1952-53 (Benson, 1962) and the British North Greenland Expedition in 1958 (Bull, 1958)  
21 which studied the accumulation rate in northern Greenland. But there had been no stable water  
22 isotope studies in the central part of northern Greenland before. Fischer et al. (1998c) and  
23 (Schwager, 2000) present the first results from  $\delta^{18}\text{O}$  values of some of the NGT records.

24 Using the updated accumulation rates of the (compared to Friedmann et al., 1995; Schwager,  
25 2000) NGT, it was possible to show that the area of lower accumulation rates is much larger  
26 than expected before, which has an influence on the outlet glaciers (Weißbach et al., 2015).

27 The NGT ice cores offer for the first time the possibility to study the spatial and temporal  
28 variability of stable oxygen isotope records from northern Greenland. Furthermore, they allow  
29 the analysis of the common spatial stable water isotope signal in northern Greenland by stacking  
30 the individual records to significantly reduce the isotopic noise that is present in a single record  
31 due to local peculiarities.

32 The main objectives of this study are 1) to investigate the spatial variability of  $\delta^{18}\text{O}$  in northern  
33 Greenland using this new set of  $\delta^{18}\text{O}$  data and to evaluate the influence of isotopic noise on a

1 single record, 2) to assess whether stable water isotope records from sites with low  
2 accumulation rates can be interpreted as climate signals, 3) to present a new robust stacked  $\delta^{18}\text{O}$   
3 record for northern Greenland covering the past millennium, and 4) to interpret this record in  
4 terms of paleoclimate with respect to temporal variability and relation to large-scale climate  
5 information from other proxy records.

6

## 7 **2 Material and Methods**

8 The ice cores presented here were drilled during the NGT from 1993 to 1995. In total, 13 ice  
9 cores (B16-B23, B26-B30) from 12 different sites (Table 1, Fig. 1) were drilled along the  
10 traverse route. The ice cores cover the last 500-1000 years. The drillings were accompanied by  
11 extensive surface snow studies (e.g. Schwager 2000).

12 B21 and B23 as well as B26 to B30 are located on ice divides (Fig. 1) while B16-B20 were  
13 drilled east of the main ice divide. The NGRIP core (North Greenland Ice Core Project  
14 Members 2004) was drilled 14.5 km northwest of B30 following the main ice divide and is  
15 therefore included in this study.

16 Before analyzing the stable water isotopes, a density profile of each core was measured. To do  
17 so, the single core segments (approximately 1 m long) were weighed in the field. Additional  
18 higher-depth resolution density records were determined using gamma-absorption  
19 measurements in the AWI cold lab (Wilhelms, 1996). Finally, in 2012 density of the first 70 m  
20 of the three cores B19, B22 and B30 was analysed by X-ray computer tomography (X-CT,  
21 Freitag et al., 2013).

22 An exponential function fitted to the data taking into account all three types of density data with  
23 same respect was used to calculate water equivalent (w. eq.) accumulation rates and to  
24 synchronize the cores.

25 Selected parts of B30 were also analyzed for electrolytic conductivity using high resolution  
26 continuous flow analysis (Kaufmann et al., 2008).

27 For the isotopic measurements the ice was cut in samples of 1-5 cm depth resolution,  
28 corresponding to 2-10 samples per year. Most of the ice was sampled with 2-2.5 cm depth  
29 resolution. Only at the uppermost parts of the core samples were cut with lower depth resolution  
30 (up to 5 cm). For some meters of special interest a resolution of 1 cm was used. After melting  
31  $\delta^{18}\text{O}$  was determined using mass spectrometers type Delta E und S from Finnigan MAT in the  
32 AWI laboratory with uncertainties less than 0.1 ‰ as determined from long-term  
33 measurements. The cores B27 and B28 were drilled at the same site. Parts of the core B27 (8.25-

1 11.38 m water equivalent (w. eq.)), corresponding to AD 1926-1945) got lost, and were  
2 replaced by the record from B28. For the other parts, the mean of both dated cores was  
3 calculated to generate one isotope record for this site.

4 Six of the NGT cores (B16, B18, B20, B21, B26 and B29) were already dated up to a certain  
5 depth by annual layer counting (using density, major ions or  $\delta^{18}\text{O}$ ) in prior studies (e.g. Fischer  
6 and Mieding, 2005; Fischer et al., 1998a; Fischer et al., 1998b; Schwager, 2000). Depending  
7 on the availability of data and differences in snow accumulation rates the dating quality of these  
8 cores varies between 1 and 5 years accuracy. For the other NGT cores annual layer counting  
9 was not possible due to the very low accumulation rates ( $<100 \text{ [kg m}^{-2} \text{ a}^{-1}]$ ). To achieve the  
10 same dating quality for all NGT cores for better comparison and to apply the dating on the  
11 whole core length, we used a new dating procedure for all cores. From density corrected (w.  
12 eq.) high resolution electrical conductivity profiles (Werner, 1995; Wilhelms, 1996) and  $\text{SO}_4^{2-}$   
13 -concentration profiles for B16, B18, B21 (Fischer et al., 1998a, b), B20 (Bigler et al., 2002)  
14 and electrolytic conductivity profile (B30), distinct volcanic horizons were identified and used  
15 as match points to synchronize the cores (Table 2). Some of the volcanic eruptions show a more  
16 pronounced signal in the Greenlandic ice than others. Thus not all eruptions could be identified  
17 in every record.

18 Between match points, the annual dating was assigned assuming a constant snow accumulation  
19 rate. If a volcanic match point could not be clearly identified in an ice core, the next time marker  
20 was used to calculate the mean accumulation rate. Below the deepest volcanic match point, the  
21 last calculated accumulation rate was extrapolated until the end of the core. As the cores were  
22 drilled only in the upper part of the ice sheet (up to 100-175 m depths) layer thinning was not  
23 taken into account.

24

## 25 **3 Results and discussion**

### 26 **3.1 Depth-age models and snow accumulation rates**

27 The last millennium was a volcanically active time (Sigl et al., 2013). The volcanic aerosols  
28 deposited on the Greenland ice sheet can be used as time markers. The depths of peaks in  
29 conductivity and sulfate concentration attributed to certain volcanic horizons are given in Table  
30 2 as used for our dating approach.

1 During the last 500 years, the time period between two detectable eruptions at NGT sites does  
2 not exceed 100 years for all the cores. This leads to a dating uncertainty for each core smaller  
3 than 10 years compared to the annually counted timescales (Mieding, 2005; Schwager, 2000),  
4 minimal at the matching points. The three youngest volcanic reference horizons (Katmai,  
5 Tambora and Laki), the eruption from 1257 AD (Samalas, Lavigne et al., 2013), and 934 AD  
6 (Eldgia) were found in all cores, whereas the other eruptions could not be clearly identified in  
7 every ice core. We could not find a common pattern (e.g. distance, strength of the eruption)  
8 whether or not volcanic horizons could be observed in all records.

9 This already indicates a high spatial variability within the study region related to significant  
10 influences of local to regional peculiarities (e.g. wind drift or sastrugi formation). An overview  
11 of the resulting mean accumulation rates for the entire core lengths for all NGT drilling sites as  
12 well as the respective ranges are given in Table 3. According to our dating, the cores reaching  
13 furthest back in time are B18, B19 and B20, covering more than the last 1000 years. These  
14 northeasterly cores have the lowest accumulation rates with values below  $100 \text{ kg m}^{-2} \text{ a}^{-1}$  (B19:  
15  $94 \text{ kg m}^{-2} \text{ a}^{-1}$ , B20:  $98 \text{ kg m}^{-2} \text{ a}^{-1}$ ), whereas the highest mean accumulation rate is found for  
16 B27/28 in the southwest of our study region with  $180 \text{ kg m}^{-2} \text{ a}^{-1}$ . Generally, the accumulation  
17 rate decreases from the sites located on the main ice divide in the south west of the study area  
18 to the north east.

19 The observed range of accumulation at one single site is highest for the southwestern cores  
20 (B30 and B29) ranging between 137 and  $161 \text{ kg m}^{-2} \text{ a}^{-1}$  (B29). Lowest values are found for the  
21 cores east of the main ice divide (e.g. B17, B18 and B19) ranging between 113 and  $119 \text{ kg m}^{-2}$   
22  $\text{a}^{-1}$  (B17).

23 The length of the records varies depending on accumulation rate and total length of the core.  
24 The longest records are from B19 (back to 753 AD) and B20 (back to 775 AD). The following  
25 comparisons of the individual records refer to the longest common time window (1505-1953  
26 AD). Although diffusion is known to change isotopic values in the snow, in this study the data  
27 were not corrected for diffusion effects. While diffusion length is in the range of annual layer  
28 thickness, diffusion might be affect the absolute difference in isotope content of neighboring  
29 years but the mean over 11 or 30 years will not be affected.

### 30 **3.2 Regional variability of $\delta^{18}\text{O}$ in northern Greenland**

31 Annual mean  $\delta^{18}\text{O}$  records of the NGT cores are displayed in Fig. 2. Table 4 summarizes the  
32 main  $\delta^{18}\text{O}$  characteristics of each core.

1 The lowest mean  $\delta^{18}\text{O}$  values ( $\sim -37\text{‰}$ ) in northern Greenland (B16-B18) and maybe the lowest  
2 in Greenland are found east of the main ice divide and north of the summit, but not at the summit  
3 as might be expected. Also the lowest firn temperatures were measured at B16-B18 (Tab. 4).  
4 This is in contrast to the findings of Ohmura (1987), who suggested for this region temperatures  
5 similar to summit.

6 Generally, the cores located east of the main ice divide show lower mean  $\delta^{18}\text{O}$  values than those  
7 located on the ice divide (Fig. 3a). For instance, B29, and B30 are on similar altitude and  
8 latitudes as B16 and B17 but show significantly heavier values (Fig. 3a).

9 Fig. 4 indicates that accumulation, latitude and altitude may have minor impact on the  $\delta^{18}\text{O}$   
10 values here. One possible explanation would be additional moisture isotopically depleted  
11 during the transport from rather northern directions.

12 The cores more to the north (B19-B22) were drilled at lower altitude and therefore record  
13 different climate signals (i.e. from lower air masses) compared to the high altitude ice cores  
14 that, in turn, record a more smoothed signal of higher atmospheric layers. Similar effects were  
15 observed e.g. in Svalbard (Isaksson et al., 2005), even though in considerably lower altitudes  
16 compared to Greenland.

17 The maximum difference in mean  $\delta^{18}\text{O}$  values of individual ice cores is 3.3 ‰ (highest mean  
18  $\delta^{18}\text{O}$  in B26:  $-33.86\text{‰}$ , lowest mean  $\delta^{18}\text{O}$  in B17:  $-37.13\text{‰}$ ). The standard deviation (SD) for  
19 the annual mean values within each core in the common time window (1505 - 1953 AD) is  
20 lowest for B16 (0.99 ‰) and highest for B18 (1.44 ‰). We found no general relation between  
21 accumulation rate and standard deviation of the  $\delta^{18}\text{O}$  values for all individual cores, even though  
22 the northern cores with generally lower accumulation rates show higher standard deviations  
23 than the southern cores.

24 The correlation coefficients between the annual  $\delta^{18}\text{O}$ -records of individual ice cores are  
25 relatively small ( $r = 0.1$  to  $0.36$ ,  $p < 0.05$ ). This can be partly explained by the fact that the 13  
26 northern Greenland (NG) drilling sites (12 NGT and NGRIP) are up to 680 km apart from each  
27 other. In other studies where correlated cores are drilled closer together, at one drill site, they  
28 found higher correlation coefficients (e.g. at GRIP  $r = 0.41$ - $0.55$  (White et al., 1997) or at  
29 NEEM  $r \sim 0.54$  (Masson-Delmotte et al., 2015)). The strongest correlations are found for the  
30 cores from the southwest (B26-B30) and the lowest for those from the northeast (B19, B20).  
31 There is a significant linear relationship between the distance between the core sites and their  
32 annual  $\delta^{18}\text{O}$  correlation coefficient ( $r = -0.44$ ,  $p < 0.05$ ). However, it is not always true that the  
33 cores with smallest distance between them have the highest correlations.

1 For smoothed values (11 year running mean) the correlation coefficients between the  $\delta^{18}\text{O}$   
2 records are only slightly higher. Only 50 % of the combinations have coefficients higher than  
3 0.3, and 14 % are lower than 0.1. This indicates an important influence of regional site to site  
4 differences. Variability in  $\delta^{18}\text{O}$  is dependent on local (e.g. wind), regional (e.g. position on the  
5 ice sheet) and large-scale (e.g. circulation patterns) processes. Even adjacent cores may differ  
6 considerably according to snow drift (Fisher et al., 1985). One further reason for the rather low  
7 correlations may be attributed to dating uncertainties.

8 From Fig. 2, we compare our individual NGT  $\delta^{18}\text{O}$  records to other published Central to North  
9 Greenland (GRIP, GISP2, NGRIP)  $\delta^{18}\text{O}$  time series. Prominent decadal-scale maxima and  
10 minima occurred mostly isochronally. However, specific events such as warm periods around  
11 1420 AD or 1920-30 AD or a cold period in the 17<sup>th</sup> century are more pronounced in the NGT  
12 cores compared to summit records.

13 In Fig.2 is also obvious that some records show faster changes between warmer and colder  
14 events (e.g. GRIP, B30 and B26), while others (e.g. B17-B21) remain longer at values higher  
15 or lower than their mean (Fig. 2). The longest warm period (compared to the mean of whole  
16 core length) is found in B19 (with 37 subsequent years warmer than the mean), while B17 has  
17 the longest cold period (28 subsequent years colder than mean). GRIP, B26, and B27/28 show  
18 a higher frequency with a maximum of about ten subsequent warmer or colder years. A  
19 frequency analysis on 11-year running mean smoothed data supports these findings. B18-B21  
20 and B29 show much longer main periods (117-248 a) than B16-B17 and B22-B30 (besides  
21 B29, 81-39 a).

22 In general, the first half of the last millennium was characterized by longer warm or cold  
23 anomalies than the second half and records with more rapid fluctuations are from summit and  
24 the main ice divide, while those cores drilled east of the divide have longer periods of positive  
25 or negative anomalies. We conclude that east of the divide, the climate conditions are not as  
26 variable and therefore the annual  $\delta^{18}\text{O}$  signal is of greater persistence.

27 The east-to-west difference is also expressed by the dependency of  $\delta^{18}\text{O}$ -values on longitude  
28 (Fig. 4). This is in line with results from Box (2002), who found that there is often an opposite  
29 trend in air temperatures in east and west Greenland. The antiphase of temperature records from  
30 east and west Greenland is may be explained by the importance of different weather regimes  
31 (e.g. Ortega et al., 2014).

32 The range in  $\delta^{18}\text{O}$  in the different cores is different, too. Cores drilled in the northeast that are  
33 characterized by the lowest accumulation rates have the highest standard deviations (SD) in



1  $\delta^{18}\text{O}$ , which can be partly explained by the fact that a smaller number of accumulation events  
2 scatters easier.

3 We investigated the relationship between the altitude, latitude and longitude of the drilling sites  
4 and the mean  $\delta^{18}\text{O}$  values (Fig. 4a, b, c), which are when considering all records, statistically  
5 significant ( $p < 0.05$ ) only for longitude and latitude. Regarding their snow accumulation rate we  
6 differentiate two groups: I) cores with accumulation rates lower than  $145 \text{ kg m}^{-2} \text{ a}^{-1}$  mainly  
7 located east of the main ice divide (B16-B21 and B23) and II) cores with higher accumulation  
8 rates (B22, B26-B30 and NGRIP). We find heavier  $\delta^{18}\text{O}$  ratios for sites with higher  
9 accumulation rates (Fig. 4d). The relationship is weak but becomes stronger for higher  
10 accumulation rates. Buchardt et al. (2012) noted that the relationship between accumulation  
11 rate and  $\delta^{18}\text{O}$  is not distinct for Greenland. Furthermore Buchardt et al. (2012) found that the  
12 sensitivity of  $\delta^{18}\text{O}$  changes to accumulation rate is smallest in northeast Greenland (North  
13 Central and North 1972), which is in agreement with our findings.

14 Among the factors influencing the mean isotopic composition, the longitude has the strongest  
15 impact ( $R^2 = 0.56$ ) which become clearest looking only at the data of group I ( $R^2 = 0.93$ ). Figure  
16 4 c) shows the clear east-to-west gradient in the mean  $\delta^{18}\text{O}$  values in northern Greenland.

17 If separating between group I (“East”) and group II (“Divide”) there is a strong altitude effect  
18 ( $R^2 = 0.93$  and  $0.78$ ) in the data, too.

19 These patterns may be explained by different atmospheric circulation conditions allowing  
20 additional moisture from other sources to reach the region east of the ice divide. This is  
21 supported by the finding of Friedmann et al. (1995) who suppose based on data from B16 to  
22 B19 that northeast Greenland receives more moisture from local sources as the Greenlandic  
23 Sea, Atlantic Ocean and the Canadian Wetland, in particular during summer.

24 We found lighter  $\delta^{18}\text{O}$  values in the southern and eastern part of northern Greenland in contrast  
25 to the general ideas of Dansgaard (1954), who expected lighter values northward. That we do  
26 not find the lightest values north is a consequence of different factors in northern Greenland  
27 that out balance each other. More to the north, where we would expect lighter  $\delta^{18}\text{O}$  values, the  
28 altitude in northern Greenland is decreasing which causes heavier  $\delta^{18}\text{O}$  values (Fig. 1). As  
29 Johnsen et al. (1989) did, multiple linear regression becomes necessary.

30 Applying this approach to our data, we find  $\delta(\delta^{18}\text{O})/(\delta(\text{latitude})) = -0.30 (+/-0.40) \text{ ‰/degree}$  and  
31  $\delta(\delta^{18}\text{O})/\delta(\text{altitude}) = -0.0035 (+/- 0.0024) \text{ ‰/m}$ . The regression residuals are linearly related to  
32 longitude as well as accumulation rate.

1 Generally, we found correlations to altitude, latitude and longitude but the out balancing effects  
2 because of the special topography in northern Greenland have to be taken into account.

3 To study the regional-scale patterns of common variability of all annual  $\delta^{18}\text{O}$  records, we  
4 performed a principal component analysis (PCA). All calculations are done for the largest  
5 common time window of all cores (1505-1953 AD). Other time periods were used as well, and  
6 they show similar results.

7 Only the first two principal components (PC1 and PC2) are above the noise level. The first two  
8 eigenvectors of the isotopic time series explain 34.1 % of the total variance (PC1: 21.8 %, PC2:  
9 12.3 %). The PC1 is similar to the mean of all records ( $r = 0.97$ ,  $p \ll 0.01$ ). It was not possible  
10 to assign PC2 to any climatic relevant signal. The other PCs are dominant in one or two records  
11 but are not significant for the total variance of the entire dataset. The loading patterns show a  
12 homogeneous pattern for EOF1 and a bipolar (west-east) result for EOF2.

13 To summarize, the spatial differences in mean  $\delta^{18}\text{O}$  values in northern Greenland can be largely  
14 explained by the influence of the topography of the ice sheet on the regional climate system.  
15 The main ice divide influences the pathways of air masses causing lower accumulation rates in  
16 the east.

17 We assume that the temporal variability in a stacked NG  $\delta^{18}\text{O}$  record represents past  
18 temperature development.

### 19 **3.3 The northern Greenland $\delta^{18}\text{O}$ -stack and its paleoclimatic significance**

20 Stable water isotope ratios in ice are widely used as a proxy for air temperature (Dansgaard,  
21 1964; Johnsen et al., 1995; Jouzel et al., 1997b). The comparison to direct air-temperature  
22 observation data and proxy data allows to assess the quality of the proxy in terms of paleo-  
23 climatological interpretation.

24 To reduce the noise in the single  $\delta^{18}\text{O}$  records, we calculated a stacked record by averaging the  
25 13 annual NG  $\delta^{18}\text{O}$  records in their overlapping time periods (NG-stack, Fig. 5). Before  
26 stacking, all records were centred and normalized regarding their common time window (1505-  
27 1953 AD). The SD of the NG-stack (0.44 for 1505-1953 AD) is less than half of the SD in  
28 annual  $\delta^{18}\text{O}$  records of the individual cores. Also Vinther et al. (2010) make clear that stacking  
29 is important to improve the signal-to-noise ratio in low accumulation rate areas. Local drift  
30 noise would account for half of the total variance in single-site annual series (Fisher et al.,  
31 1985). As the NG-stack before 1000 AD is based on only four records (< 25% of the total core  
32 numbers), we decided to focus in the following only on the time period after 1000 AD.

1 As the NG-stack is a result of 13 ice cores over a large area we assume its regional  
2 representativity.

3 To investigate the relationship of the NG-stack with air temperature, we used monthly  
4 meteorological observations from coastal southwest Greenland sites and Stykkisholmur in  
5 Northwest Iceland available from the Danish Meteorological Institute (DMI-  
6 <http://www.dmi.dk>; 1784-1993 AD) and the Icelandic meteorological office  
7 (<http://en.vedur.is/>; back to 1830 AD), respectively. We selected only the Greenlandic  
8 temperature records longer than 200 years for our study even though they are in large distance  
9 (706-2206 km).

10 The correlation coefficients between the NG-stack and these air temperature records are shown  
11 in Table 5. Dating uncertainties are taken into account by comparing 5 year running means. The  
12 NG-stack shows low but significant ( $p < 0.001$ ) correlations to the air temperatures at all sites  
13 (Tab. 5).

14 The strongest correlation with annual mean temperature was found for the merged station data  
15 at Greenland's southeast coast ( $r = 0.51$ ), and the temperature reconstruction for the North  
16 Atlantic Arctic boundary region of Wood et al. 2010 ( $r = 0.55$ ); the lowest was found for  
17 Qaqortoq ( $r = 0.39$ ) also in the south of Greenland (Tab. 5). For Stykkisholmur the correlation  
18 is in the range of the Greenlandic ones ( $r = 0.41$ ). Slightly higher correlations are obtained by  
19 comparing the NG-stack to seasonal data. Except for Ilulissat, winter months (DJF) show  
20 weaker correlations; spring (MAM) and summer (JJA) months show stronger correlations to  
21 the NG-stack.

22 Comparably low correlations between annual  $\delta^{18}\text{O}$  means and measured temperatures from  
23 coastal stations are also reported for the NEEM record (Steen-Larsen et al., 2011).

24 However, the rather low correlation coefficients might underestimate the real regional  $\delta^{18}\text{O}$ -  
25 temperature relations because of different reasons.

26 We expect that the most important reasons are the large distances and the difference in altitude  
27 (i.e. more than 2,000 m) between drill sites and the meteorological stations, which let them  
28 receive different atmospheric signals. The stations are located at the coast and are in turn also  
29 likely influenced by local factors as the occurrence of sea ice.

30 One other aspect might be the seasonality as argued by Steen-Larsen et al. (2011) for the NEEM  
31 site. The snow fall in northern Greenland maybe seasonally unevenly distributed. However, it  
32 is not possible to generate sub-annual data for northern Greenland ice cores due to low  
33 accumulation rates. We find a tendency to stronger correlation between the annual  $\delta^{18}\text{O}$  and

1 summer (JJA,  $r = 0.35-0.51$ ) and spring (MAM,  $r = 0.36-0.62$ ) temperatures for most of the  
2 stations. This points to a higher proportion of summer snow in the annual accumulation in  
3 northern Greenland, too. SON has slightly weaker correlation coefficients ( $r = 0.31-0.5$ ) while  
4 DJF is only significant for Illulisat and the merged southern station.

5 Also regional noise factors such as wind drift and sastrugi formation as well as uncertainties in  
6 ice core dating and the usage of very old observation data have to be taken into account.

7 In summary, we consider the northern Greenland  $\delta^{18}\text{O}$  stacked record as a reliable proxy for  
8 annual temperature for northern Greenland. The regional representativeness of the NG-stack is  
9 supported by the general similarity to the NEEM  $\delta^{18}\text{O}$  record (Masson-Delmotte et al., 2015)  
10 for the period 1724-1994 AD. We found a strong correlation between both records ( $r = 0.83$  for  
11 30-year running mean). Even single events such as the highest values in 1928 AD and the 1810-  
12 1830 AD cooling occur in both records.

13 Although the NG-stack record shows some correlation with temperature data from coastal  
14 Greenland sites, it remains an open question, how the NG-stack  $\delta^{18}\text{O}$  variations can be  
15 converted to absolute temperature changes within North-East Greenland during the last  
16 millennium. For more than 30 years such conversion of isotopic time series of Greenland ice  
17 cores was based on a modern analogue approach taking the observed spatial  
18 isotope/temperature gradient of  $0.67 \pm 0.2 \text{‰ } ^\circ\text{C}^{-1}$  (Dansgaard, 1964; Johnsen et al., 1989) as  
19 a valid calibration for converting isotope records of Greenland ice cores into temperature  
20 changes (e.g. Grootes et al., 1993). The strong confidence of glaciologists into this approach  
21 came principally from two observations. 1) Over both polar ice sheets, the spatial correlation  
22 between modern isotope and annual mean temperature is very high and significant. 2) This  
23 empirical observation was theoretically understood as a consequence of a Rayleigh rainout  
24 system controlling the isotopic composition of meteoric water.

25 However, for the Greenland area this long time accepted approach has been challenged during  
26 the last decade. Two entirely independent analytic techniques, one based on the numerical  
27 interpretation of borehole temperatures (e.g. Dahl-Jensen et al., 1998) and the other based on  
28 the occlusion process of gases into the ice (e.g. Buizert et al., 2014; Severinghaus et al., 1998)  
29 allow a direct temperature reconstruction at least for some periods of the past. Consistently both  
30 methods point to much lower temporal  $\delta^{18}\text{O} \text{ T}^{-1}$  slopes ranging between  $0.4-0.3 \text{‰ } ^\circ\text{C}^{-1}$  (Jouzel  
31 et al., 1997a). Consequently they indicate a much higher temperature variability in Greenland  
32 during the last glacial period. For the period of the last 9000 years the Greenland average  
33 Holocene isotope-temperature relationship has been estimated to be  $0.44-0.53 \text{‰ } ^\circ\text{C}^{-1}$  again

1 substantially lower as the modern spatial gradient (Vinther et al., 2009). However, as all these  
2 studies cover much longer time periods as compared to our NG-stack records, no firm  
3 conclusion can be drawn from these studies about an appropriate isotope-temperature  
4 relationship for the last millennium.

5 Along the NGT firn temperature measurements in about 15 m depth had been done (Tab. 4).  
6 But due to their small range of about 2 K difference it is difficult to reassess the general  
7 Greenland isotope temperature relationship from Johnsen et al. (1989) from the NGT data,  
8 solely. Schwager (2000) added data from Dansgaard et al. (1969) from along the EGIG traverse,  
9 which was also used in Johnsen et al. (1989), to expand the temperatures range to derive a more  
10 reliable isotope-temperature gradient. This calculated gradient of  $0.7 \pm 0.2 \text{ ‰ } ^\circ\text{C}^{-1}$  is within  
11 the gradient uncertainty range given by Johnsen et al. (1989). Using our updated NGT dataset  
12 we get the same results.

13 If we apply the spatial isotope/temperature gradient of  $0.7 \text{ ‰ } ^\circ\text{C}^{-1}$  from Schwager (2000) for  
14 the range of isotope variations ( $-1.4 \text{ ‰}$  to  $2.5 \text{ ‰}$ ) of the NG-stack record, the isotope data would  
15 translate into temperature changes of  $-2.0 \text{ }^\circ\text{C}$  to  $3.6 \text{ }^\circ\text{C}$  (5.6 K) within the last millennium.  
16 However, applying instead a temporal gradient of  $0.48 \text{ ‰ } ^\circ\text{C}^{-1}$  as suggested by Vinther et al.  
17 (2009) results in possible temperature changes of  $-2.9 \text{ }^\circ\text{C}$  to  $5.2 \text{ }^\circ\text{C}$  (8.1 K) within the last 1000  
18 years. Using the most recent temporal glacial-interglacial isotope-temperature gradients  
19 reported by Buizert et al. (2014) would result in comparable temperature changes. If using the  
20 NEEM gradient of  $1.1 \pm 0.2 \text{ ‰ } ^\circ\text{C}^{-1}$  (Masson-Delmotte et al., 2015), which is valid for 2007-  
21 1979 AD in the area of NEEM, the resulting temperature range of the NG-stack is with  $-1.3$  to  
22  $2.3 \text{ }^\circ\text{C}$  (3.6 K) a bit smaller than compared to the Johnsen or Schwager gradient. Nevertheless,  
23 the resulting temperature ranges are larger than expected (e.g. Dahl-Jensen et al., 1998) which  
24 is an additional argument not to calculate absolute temperatures from the NG-stack with the  
25 given gradients.

26 We conclude that any conversion of the NG-stack isotope record into absolute temperature  
27 variations during the last millennium is highly uncertain. Thus, for the following part of the  
28 manuscript, we will refer to NG-stack isotope anomalies as relative temperature changes in  
29 terms of “warmer” (i.e. isotopically enriched) and “colder” (isotopically depleted), only, but  
30 refrain from converting our ice core data into absolute temperature changes.

31 To assess regional differences within northern Greenland, stacks of subsets of cores will be  
32 discussed in terms of interpretation as a temperature proxy. As illustrated in Fig. 4, we  
33 differentiate two different types of cores, cores drilled on the ice divide and cores drilled east  
34 of the ice divide. Accordingly, in Fig. 5 the overall northern Greenland  $\delta^{18}\text{O}$  stack used in this

1 study is compared to a stack of the cores of lower accumulation rate drilled east of the main ice  
2 divide (B16, B17, B18, B19, B20, B21 and B23) (“stack east”) and a stack of those on the ice  
3 divide (B22, B26, B27, B29, B30 and NGRIP) (“stack divide”) (Fig. 5).

4 Even though there is a similar overall trend, the three records show differences in amplitude  
5 and timing of warm and cool events. The correlation between the two sub-stacks is rather low  
6 ( $r = 0.71$  of 30 year running means). In the 11<sup>th</sup> and 12<sup>th</sup> centuries, we observe a quasi-anti-  
7 correlation between stack “East” and stack “Divide”. Even during well-known climate events  
8 such as the Medieval Climate Anomaly (MCA, 950 - 1250 AD, Mann et al., 2009), the Little  
9 Ice Age (LIA, 1400 - 1900, Mann et al., 1998) and the Early Twentieth Century Warming  
10 (ETCW 1920 - 1940 AD, Semenov and Latif, 2012), there are significantly different  $\delta^{18}\text{O}$   
11 patterns. For example, stack “Divide” shows colder temperatures during 1000-1200 AD. Also,  
12 during the 16<sup>th</sup> century we notice substantial differences between the two sub-stacks. In stack  
13 “East” events like the 1420 AD or the first part of the LIA show a higher amplitude.

14 The stack “East” has a higher correlation to the total NG-stack ( $r = 0.96$ ) compared to stack  
15 “Divide” ( $r = 0.68$ ) for the period 994-1994 AD. Looking at the time period 1505-1993 AD  
16 with a high number of cores included in both sub-stacks, the correlation coefficients to the total  
17 NG-stack are almost equal (stack “East”:  $r = 0.95$ , stack “Divide”:  $r = 0.90$ ,  $p < 0.1$ ). Here, both  
18 records reflect the mean changes in  $\delta^{18}\text{O}$  for northern Greenland. Differences before 1505 AD  
19 may be artefacts of low core numbers even though regional differences in climate conditions  
20 cannot be ruled out.

21 We consider the NG-stack as a climate record that displays the overall climate variation  
22 independent of local influences as topography or accumulation rate. In contrast, results from  
23 studies with only one record become less spatially representative, as they may be affected by a  
24 lower signal-to-noise ratio and a higher influence of other local non-climate effects.

### 25 **3.4 Last millennium climate from a stacked NG $\delta^{18}\text{O}$ record in relation to other** 26 **proxy records and possible forcing factors**

27 The NG-stack covers the time between 753 AD and 1994 AD (Fig. 5). For a better visualisation  
28 of decadal to centennial scale variability a 30-year running mean is added. The running mean  
29 shows the warmest period around 1420 AD and the coldest in about 1680 AD. The isotopically  
30 warmest single year during the last 1000 years in northern Greenland was 1928 AD, whereas  
31 1835 AD was the coldest.

1 Distinct decadal- to centennial-scale warm and cold anomalies can be detected in the stacked  
2 (Fig. 5) as well as individual  $\delta^{18}\text{O}$  records (Fig. 2) and coincidence to well-known climate  
3 anomalies (MCA, LIA, ETCW, marked in Fig. 5).  
4

5 We find a pronounced warm period from 850 to 1100 AD, which has its maximum between  
6 900 and 1000 AD. This is about 100 years earlier than the described MCA in Mann et al. (2009).  
7 The warm period is followed by a quasi-periodical change of warm and cold phases observed  
8 approximately every 60 to 80 years until about 1600 AD. During this phase, the most distinct  
9 warm period is observed around 1420 AD.

10 A longer period of cold temperatures occurred during the 17<sup>th</sup> and early 19<sup>th</sup> century and was  
11 already attributed to the LIA by a prior NGT study that used only 4 cores (B16, B18, B21 and  
12 B29, Fischer et al., 1998c). A cold period in northern Greenland corresponding to the LIA is  
13 later than reconstructed for the entire Northern Hemisphere by Mann et al. (1998), with lowest  
14 values during 1620-1780 AD and in the first half of the 19<sup>th</sup> century. Interestingly, the warmest  
15 mean values of the last 1000 years at 1420 AD lie within the timeframe of LIA.

16 A distinct, but compared to other periods not outstanding, warm event in the early 20<sup>th</sup> century  
17 corresponds to the ETCW. Since the 1870s AD, the values are above the 1000-year mean. At  
18 the end of the 20<sup>th</sup> century, the temperature stagnates at a high mean level. However, as the  
19 NGT cores were drilled between 1993 and 1995 AD, the warmest years of the recent decades  
20 (Wood et al., 2010) are not included in our record.

21 For the NG-stack as well as most of the individual NGT cores the isotopically warmest periods  
22 besides the 1420 AD event were in the 10<sup>th</sup> and 20<sup>th</sup> centuries, in particular between 1900 and  
23 1950 AD. These years are even warmer than the most recent years covered by the NGT cores  
24 (i.e. the 1980s).

25 To set the results in an Arctic-wide context we compare our northern Greenland temperature  
26 record (NG-stack) to ice-core records from the Russian Arctic (Akademii Nauk – AN, Opel et  
27 al., 2013), Canada (Agassiz Ice Cap – Agassiz, Vinther et al., 2008), Svalbard  
28 (Lomonosovfonna - Lomo, Divine et al., 2011) and south Greenland (Dye3, Vinther et al.,  
29 2006b) as well as a multi-proxy reconstruction of annual Arctic SAT (Arctic2k, PAGES 2k  
30 Consortium, 2013, Fig. 6) that cover our time period.

31 Note that some of these time series (Agassiz, Arctic2k) are also stacked records with a wider  
32 regional representativeness, whereas others are single records (Dye3, AN, Lomo), which

1 influences the strength of correlation due to different signal-to-noise ratios. For the discussion  
2 of the temperature record, we concentrate on the smoothed values (30-year running means).  
3 The strongest correlations to our NG-stack are found for the Agassiz and Arctic2k records ( $r =$   
4  $0.58$  and  $0.66$ , respectively). For the latter, we have to consider that some of the NGT cores  
5 (B16, B18 and B21 on the old time scale) are used to generate this multi-proxy record. In total,  
6 59 records including 16 ice cores were used. NGT cores represent only 3 out of these 59  
7 records. The correlation coefficient between the stacked anomalies of B16, B18 and B21 and  
8 the Arctic2k temperature is small ( $r = 0.24$ ) so we can assume that the NGT records do not  
9 dominate the reconstruction.

10 We conclude that a good correlation between the NG-stack and the Arctic2k record show that  
11 the temperature in northern Greenland follows in general the Arctic-wide mean temperature.  
12 The Lomonosovfonna record is interpreted as a winter record and has only a weak correlation  
13 to the NG-stack ( $r = 0.22$ ). More summer snow in northern Greenland compared to  
14 Lomonosovfonna could be one possible explanation for the weak correlation between both  
15 records. While for the other drill sites we have comparable  $r$ -values for both substacks as for  
16 the NG-stack, the Lomo has a stronger correlation to stack “East” ( $r = 0.2$ ) than to stack  
17 “Divide” ( $r = -0.12$ ) which supports the argument of different moisture sources or seasonal  
18 distribution of snow fall in north-east of Greenland.

19 The Lomonosovfonna, Akademii Nauk and Arctic2k records show significantly more enriched  
20  $\delta^{18}\text{O}$  values during the MCA. However, smaller events of abnormal warm temperatures during  
21 the MCA are observed for Agassiz and Dye3. Our NG-stack shows warmer values earlier than  
22 the MCA time period given by Mann et al. (1998). We conclude that further north in the Arctic  
23 the warm events during MCA may be less pronounced or earlier in timing.

24 The Lomonosovfonna and Arctic2k records show a dominant cold period during the LIA from  
25 1580 to 1870 AD. Also, our northern Greenland as well as the Agassiz and Akademii Nauk ice  
26 cores reveal distinct LIA cooling periods in contrast to the Dye3 ice core from south Greenland.  
27 Like in our NG-stack, the cooling appears in two phases and some decades later than described  
28 by Mann et al. (2009). For the NG-stack, the younger phase (1800-1850 AD) is of minor  
29 amplitude and shorter duration.

30 Between 1920 and 1940 AD, there was a major warming period in the Arctic, known as ETCW  
31 and observed in all records shown here. Chylek et al. (2006) determined from meteorological  
32 data that the 1920–30 warming was stronger than the 1995–2005 warming. For the NG-stack  
33 and Akademii Nauk record, the ETCW was warmer than the second half of the 20<sup>th</sup> century,



1 which distinguishes them from other shown records. The ETCW is assumed to be independent  
2 of external forcing but caused by internal climate variability, in particular sea ice-atmosphere  
3 feedbacks (Wood and Overland, 2010). This let us conclude that northern Greenland may also  
4 be a good place to study forcing independent, i.e. internal, climate changes.

5 However, natural external forcing (i.e. insolation, solar irradiance and volcanic eruptions) is  
6 assumed to influence the temperature that can be studied from northern Greenland's ice cores.

7 In general, higher solar activity causes higher temperatures (as during the MCA) whereas cold  
8 periods (e.g. LIA) are dominated by lower solar activity (Ammann et al., 2007). Based on some  
9 of the NGT records (B16, B18, B21 and B29), Fischer et al. (1998c) explained most of the long-  
10 term variation in northern Greenland by changes in solar activity.

11 Volcanism causes strong negative radiative forcing (Robock, 2000). It is assumed that volcanic  
12 eruptions inject large quantities of sulfur-rich gases into the stratosphere and global climate can  
13 be cooled by 0.2-0.3 °C for several years after the eruption (Zielinski, 2000). Results from  
14 Crowley (2000) indicate that volcanism generally explains roughly 15–30 % of the variability  
15 in global temperatures.

16 Miller et al. (2012) argued that century-scale cold summer anomalies of which the LIA  
17 represents the coldest one, occur because natural forcing is either weak or, in the case of  
18 volcanism, short-lived. PAGES 2k Consortium (2013) shows that periods with strong volcanic  
19 activity correspond to a reduced mean temperature. LIA may be therefore caused by a 50 year-  
20 long episode of volcanism and kept persistently cold because of ocean feedback and a summer  
21 insolation minimum.

22 Between about 1100 and 1600 AD we observe quasi-periodic (60-80 a) cold and warm  
23 anomalies in the NG-stack which is not present in the other shown Arctic records (Fig. 6). The  
24 main period determined using Fourier decomposition between 1100 and 1600 AD for 30-year  
25 running mean smoothed values is calculated with 76.31 a.

26 The Atlantic Multidecadal Oscillation, AMO, could be one possible influence causing these  
27 low-frequency oscillations. Chylek et al. (2012) explain that the AMO is visible in  $\delta^{18}\text{O}$  values  
28 from central Greenland. As the AMO index reconstruction (Gray et al., 2004) does not cover  
29 the time between 1100 and 1600 AD, we only can speculate about an influence in that time due  
30 to the similar periodicity. For the time period 1567-1990 AD, the correlation between the NG-  
31 stack and the AMO index is weak ( $r = 0.06$ ), which might be due to the uncertainties in historical  
32 AMO data. However, since 1800 AD we observe a higher correlation coefficient ( $r = 0.66$ ,  $p <$   
33  $0.05$ ) implying a possible relation.

1 One of these warmer periods is about 1420 +/- 20 AD, an abnormal warm event which is  
2 observed in our northern Greenland record and has not been pointed out in other ice core studies  
3 before. The event is observable in all nine NGT cores covering this time (Fig. 2) as well as in  
4 NGRIP but not in the isotope records from southern Greenland as the Dye3 ice core (Fig. 6).  
5 One reason here might be the specific geographical position in the North.

6 Furthermore, we observe a difference between the Canadian and Russian Arctic regarding the  
7 1420-event. Unlike the Russian Akademii Nauk ice core, the  $\delta^{18}\text{O}$  values of the Agassiz cores  
8 from Ellesmere Island also show a trend to more enriched values in that period but not as strong  
9 as in northern Greenland.

10 The fact that the 1420 event is not clearly noticeable in other surrounding Arctic ice cores  
11 emphasizes that this event may have occurred on a smaller regional scale. However, it seems  
12 to have been of dominant influence and is also reflected in a smaller warming for the Arctic2k  
13 record (Fig. 6).

14 The spatial distribution of the 1420 event in northern Greenland is mapped in figure 3b. The  
15 event is strongest in the upper north and shows a different pattern than the  $\delta^{18}\text{O}$  anomalies of  
16 the 1920/1930 warm phase, which is also attributed to internal variability and is strongest in the  
17 northeast of Greenland.

18 Figure 10 shows possible forcing factors that might be related to the 1420 AD event. According  
19 to the reconstructed total solar irradiance record of Steinhilber et al. (2009), there was no solar  
20 maximum observed for 1420 AD that could explain the warmer temperatures in northern  
21 Greenland. As we see no forcing anomaly, we interpret the 1420-event as likely be caused by  
22 internal Arctic climate dynamics with a sea-ice-atmospheric feedback.

23 Box (2002) argued that climate variability in Greenland is linked to the North Atlantic  
24 Oscillation (NAO), volcanism and sea ice extent. NAO (Vinther et al., 2003) is calculated to be  
25 weakly reflected ( $r = -0.2$ ,  $p < 0.01$ ) in the NG-stack, similar to the results of White et al. (1997)  
26 for summit ice cores, whereas none of the single NGT records is significantly correlated  
27 ( $p < 0.05$ ) to the NAO index. The NG-stack has an increased signal-to-noise level, which is why  
28 the correlation here might be clearer than from individual records. Also, the sub-stack of the  
29 records on the ice divide (stack "Divide") as well as those east (stack "East") are significantly  
30 correlated ( $r = -0.19$  and  $-0.17$ ,  $p < 0.05$ ) to the NAO index. The cores east of the main ice divide  
31 are expected to be out of the major cyclonic track. We conclude that NAO is not of major  
32 importance for northern Greenland  $\delta^{18}\text{O}$  values.

33 Around 1420 AD, an anti-correlation between sea-ice extent in the Arctic Ocean (Kinnard et  
34 al., 2011) and the  $\delta^{18}\text{O}$  values is observed (Fig. 7). The sea-ice extent reconstruction of Kinnard

1 et al. (2011) is based on 69 proxy records of which 22 are  $\delta^{18}\text{O}$  records. Out of these 22  $\delta^{18}\text{O}$   
2 records 5 (NGRIP, B16, B18, B21 and B26) are used also in our NG-stack. We do not expect  
3 circular reasoning in the interpretation of the 1420 event because B16 and B26 do not reach the  
4 age of 1420 AD and we do not see a strong anti-correlation during any other time period.  
5 The sea ice in the Arctic Ocean shows a recession only during that warm period in northern  
6 Greenland. A shrunken sea ice extent would cause higher temperatures on a regional scale and  
7 would increase the amount of water vapour from local sources. Therefore, compared to distant  
8 sources, more isotopically-enriched moisture (Sime et al., 2013) may contribute to precipitation  
9 in northern Greenland, in particular east of main ice divide.  
10 However, we do not see any direct relationship between sea-ice extent and our NG-stack during  
11 the rest of time, which does not exclude the relationship between sea-ice extent and  $\delta^{18}\text{O}$  in  
12 northern Greenland. The used sea ice reconstruction is Arctic-wide, which means that the  
13 climatic events of regional extent, like an additional moisture source for northern Greenland's  
14  $\delta^{18}\text{O}$ , do not have to be always reflected. Nevertheless, also the recent NEEM  $\delta^{18}\text{O}$  record from  
15 northwest Greenland, shows a generally close relationship with the Labrador Sea / Baffin Bay  
16 sea ice extent (Masson-Delmotte et al., 2015; Steen-Larsen et al., 2011).

17

#### 18 **4 Conclusions**

19

20 With the full set of the NGT records, it was now for the first time possible to describe regional  
21 differences in the  $\delta^{18}\text{O}$  values in northern Greenland over the last 1000 years.

22 Because of the ice sheet topography we see a clear east-to-west difference in northern  
23 Greenland  $\delta^{18}\text{O}$  distribution. 12 % of the spatial  $\delta^{18}\text{O}$  variability is attributed to ice sheet  
24 topography. The east-to-west gradient is larger than the north-to-south gradient. We find a more  
25 pronounced persistence of warm or cold events east of the main ice divide and assume more  
26 stable climate conditions there. The eastern part is more influenced by local effects like changes  
27 in the Arctic Ocean, which has to be supported by the results of climate models. For the first,  
28 time a local warm event at 1420 +/- 20 AD was pointed out. We assume an atmosphere-sea ice  
29 feedback as one possible reason for this event.

30 Due to the shadowing effect of the main ice divide we find the lowest accumulation rates in the  
31 northeast, whereas the lowest mean  $\delta^{18}\text{O}$  values are found east of the main ice divide north of  
32 summit. The lowest  $\delta^{18}\text{O}$  mean values seem to be independent of accumulation rate.

1 We have presented a new 1000 year stacked  $\delta^{18}\text{O}$  record for northern Greenland covering 10 %  
2 of the area of Greenland. We found this NG-stack to be representative for the northern  
3 Greenland temperature.  
4 Northern Greenland  $\delta^{18}\text{O}$  represents known climatic variations of the last millennium. We see  
5 a warm MCA and can derive distinct LIA cooling from our NG-stack.  
6 The results of single site ice-core studies are likely weakened by the finding that there is only  
7 22 % common variability in the 13 NGT cores.  
8 The solar activity and internal Arctic climate dynamics are likely the main factors influencing  
9 the temperature in northern Greenland. In contrast we could not find a general cooling effect of  
10 volcanic eruptions in our data.

## 1 **Acknowledgements**

2

3 Stefanie Weißbach was financed by the “Earth System Science Research School (ESSReS)”,  
4 an initiative of the Helmholtz Association of German Research Centres (HGF) at the Alfred  
5 Wegener Institute (AWI), Helmholtz Centre for Polar and Marine Research.

6 Anna Wegner acknowledges REKLIM for funding.

7 This study contributes to the Eurasian Arctic Ice 4k project funded by Deutsche  
8 Forschungsgemeinschaft (grant OP 217/2-1 awarded to Thomas Opel).

9 Many thanks to the drill and lab team who have measured the  $\delta^{18}\text{O}$  (76.930 samples) with  
10 endurance over more than 20 years. We also thank Johannes Freitag and Katja Instenberg  
11 for high resolution (CT) density measurements, Martin Rückamp for compiling the maps,  
12 Martin Werner, Thomas Laepple and Johannes Freitag for helpful discussions that improved  
13 the manuscript and Kirstin Meyer for language check.

14 We acknowledge the constructive comments by two anonymous referees.

15 "Supplementary data are available at <http://dx.doi.org/10.1594/PANGAEA.849161>"

## 1 **References**

- 2 Ammann, C. M., Joos, F., Schimel, D. S., Otto-Bliesner, B. L., and Tomas, R. A.: Solar  
3 influence on climate during the past millennium: results from transient simulations with the  
4 NCAR Climate System Model, *P. Natl. Acad. Sci. U S A*, 104, 3713-3718, 2007.
- 5 Appenzeller, C., Schwander, J., Sommer, S., and Stocker, T. F.: The North Atlantic Oscillation  
6 and its imprint on precipitation and ice accumulation in Greenland, *Geophys. Res. Lett.*, 25, 11,  
7 1939-1942, 1998.
- 8 Bamber, J. L., Griggs, J. A., Hurkmans, R. T. W. L., Dowdeswell, J. A., Gogineni, S. P., Howat,  
9 I., Mougnot, J., Paden, J., Palmer, S., Rignot, E., and Steinhage, D.: A new bed elevation  
10 dataset for Greenland, *The Cryosphere*, 7, 499-510, doi: 10.5194/tc-7-499-2013, 2013.
- 11 Benson, C. S.: Greenland snow pit and core stratigraphic data 1952, 1953, 1954, 1955, U.S.  
12 Army Corps of Engineers Snow Ice and Permafrost Res, 70, 39-47, 1962.
- 13 Bigler, M., Wagenbach, D., Fischer, H., Kipfstuhl, J., Millar, H., Sommer, S., and Stauffer, B.:  
14 Sulphate record from a northeast Greenland ice core over the last 1200 years based on  
15 continuous flow analysis. In: *Annals of Glaciology*, vol. 35, edited by: Wolff, E. W., Int.  
16 Glaciological Soc., Cambridge, 250-256, 2002.
- 17 Box, J. E.: Survey of Greenland instrumental temperature records: 1873–2001, *Int. J. Climatol.*,  
18 22, 1829-1847, 2002.
- 19 Buchardt, S. L., Clausen, H. B., Vinther, B. M., and Dahl-Jensen, D.: Investigating the past and  
20 recent  $\delta^{18}\text{O}$ -accumulation relationship seen in Greenland ice cores, *Clim. Past*, 8, 2053-2059,  
21 doi: 10.5194/cp-8-2053-2012, 2012.
- 22 Buizert, C., Gkinis, V., Severinghaus, J. P., He, F., Lecavalier, B. S., Kindler, P., Leuenberger,  
23 M., Carlson, A. E., Vinther, B., Masson-Delmotte, V., White, J. W. C., Liu, Z., Otto-Bliesner,  
24 B., and Brook, E. J.: Greenland temperature response to climate forcing during the last  
25 deglaciation, *Science*, 345, 1177-1180, 2014.
- 26 Bull, C.: Snow accumulation in north Greenland, *J. Glaciol.*, 3, 12, 1958.
- 27 Chen, Q. S., Bromwich, D. H., and Bai, L. S.: Precipitation over Greenland retrieved by a  
28 dynamic method and its relation to cyclonic activity, *J. Clim.*, 10, 839-870, 1997.
- 29 Chylek, P., Dubey, M. K., and Lesins, G.: Greenland warming of 1920–1930 and 1995–2005,  
30 *Geophys. Res. Lett.*, 33, L11707, doi: 10.1029/2006GL026510, 2006.

1 Chylek, P., Folland, C., Frankcombe, L., Dijkstra, H., Lesins, G., and Dubey, M.: Greenland  
2 ice core evidence for spatial and temporal variability of the Atlantic Multidecadal Oscillation,  
3 *Geophys. Res. Lett.*, 39, L09705, doi: 10.1029/2012GL051241, 2012.

4 Crowley, T. J.: Causes of Climate Change Over the Past 1000 Years, *Science*, 289, 270-277,  
5 2000.

6 Dahl-Jensen, D., Mosegaard, K., Gundestrup, N., Clow, G. D., Johnsen, S. J., Hansen, A. W.,  
7 and Balling, N.: Past temperatures directly from the Greenland Ice Sheet, *Science*, 282, 268-  
8 271, 1998.

9 Dansgaard, W.: The O18-abundance in fresh water, *Geochim. Cosmochim. Ac.*, 6, 241-260,  
10 1954.

11 Dansgaard, W.: Stable isotopes in precipitation, *Tellus*, 16, 436-468, 1964.

12 Dansgaard, W., Johnsen, S. J., and Moeller, J.: One Thousand Centuries of Climatic Record  
13 from Camp Century on the Greenland Ice Sheet, *Science*, 166, 377-380, 1969.

14 Divine, D., Isaksson, E., Martma, T., Meijer, H. A. J., Moore, J., Pohjola, V., van de Wal, R. S.  
15 W., and Godtliobsen, F.: Thousand years of winter surface air temperature variations in  
16 Svalbard and northern Norway reconstructed from ice core data, *Polar Res.*, 30, 7379, doi:  
17 10.3402/polar.v30i0.7379, 2011.

18 Fischer, H. and Mieding, B.: A 1,000-year ice core record of interannual to multidecadal  
19 variations in atmospheric circulation over the North Atlantic, *Clim. Dynam.*, 25, 65-74, 2005.

20 Fischer, H., Wagenbach, D., and Kipfstuhl, J.: Sulfate and nitrate firn concentrations on the  
21 Greenland ice sheet: 1. Large-scale geographical deposition changes, *J. Geophys. Res.*, 103,  
22 21927-21930, 1998a.

23 Fischer, H., Wagenbach, D., and Kipfstuhl, J.: Sulfate and nitrate firn concentrations on the  
24 Greenland ice sheet: 2. Temporal anthropogenic deposition changes, *J. Geophys. Res.-Atmos.*,  
25 103, 21935-21942, 1998b.

26 Fischer, H., Werner, M., Wagenbach, D., Schwager, M., Thorsteinsson, T., Wilhelms, F.,  
27 Kipfstuhl, J., and Sommer, S.: Little Ice Age clearly recorded in northern Greenland ice cores,  
28 *Geophys. Res. Lett.*, 25, 1749-1752, 1998c.

29 Fisher, D. A., Reeh, N., Clausen, H. B., Fisher, D. A., Reeh, N., and Clausen, H. B.:  
30 Stratigraphic noise in time series derived from ice cores, *Ann. Glaciol.*, 7, 76-83, 1985.

1 Freitag, J., Kipfstuhl, S., and Laepple, T.: Core-scale radioscopic imaging: a new method  
2 reveals density&calcium link in Antarctic firn, *J. Glaciol.*, 59, 1009-1014, 2013.

3 Friedmann, A., Moore, J. C., Thorsteinsson, T., Kipfstuhl, J., and Fischer, H.: A 1200 year  
4 record of accumulation from northern Greenland, *Ann. Glaciol.*, 21, 19-25, 1995.

5 Gao, C., Robock, A., and Ammann, C.: Volcanic forcing of climate over the past 1500 years:  
6 An improved ice core-based index for climate models, *J. Geophys. Res.-Atmos.*, 113, D23111,  
7 doi: 10.1029/2008JD010239, 2008.

8 Gray, S. T., Graumlich, L. J., Betancourt, J. L., and Pederson, G. T.: A tree-ring based  
9 reconstruction of the Atlantic Multidecadal Oscillation since 1567 A.D, *Geophys. Res. Lett.*,  
10 31, L12205, doi: 10.1029/2004GL019932, 2004.

11 Grootes, P. M. and Stuiver, M.: Oxygen 18/16 variability in Greenland snow and ice with 10–3-  
12 to 105-year time resolution, *J. Geophys. Res. Oceans*, 102, 26455-26470, 1997.

13 Grootes, P. M., Stuiver, M., White, J. W. C., Johnsen, S., and Jouzel, J.: Comparison of oxygen  
14 isotope records from the GISP2 and GRIP Greenland ice cores, *Nature*, 366, 552-554, 1993.

15 Hanna, E., Jónsson, T., and Box, J. E.: An analysis of Icelandic climate since the nineteenth  
16 century, *Int. J. Climatol.*, 24, 1193-1210, 2004.

17 Isaksson, E., Kohler, J., Pohjola, V., Moore, J. C., Igarashi, M., Karlöf, L., Martma, T., Meijer,  
18 H. A. J., Motoyama, H., Vaikmäe, R., and Van de Wal, R. S. W.: Two ice-core  $\delta^{18}\text{O}$  records  
19 from Svalbard illustrating climate and sea-ice variability over the last 400 years, *Holocene*, 15,  
20 501 - 509, 2005.

21 Johnsen, S. J., Clausen, H. B., Cuffey, K. M., Hoffmann, G., Schwander, J., and Creyts, T.:  
22 Diffusion of stable isotopes in polar firn and ice: the isotope effect in firn diffusion. In: *Physics*  
23 *of Ice Core Records*, Hokkaido University, Place Hokkaido, 121-140, 2000.

24 Johnsen, S. J., Dansgaard, W., and White, J. W. C.: The origin of Arctic precipitation under  
25 present and glacial conditions, *Tellus Ser. B*, 41B, 452-468, 1989.

26 Johnsen, S. J., Hammer, C. U., Dansgaard, W., Gundestrup, N. S., and Clausen, H. B.: The Eem  
27 stable isotope record along the GRIP ice core and its interpretation, *Quat. Res.*, 42, 117-124,  
28 1995.

29 Jónsson, T.: the observations of Jon Thorsteinsson in Nes and Reykjavik 1820-1854, *Icel. Met.*  
30 *Office Report*, Reykjavik. 1989.



1 Jouzel, J., Alley, R. B., Cuffey, K. M., Dansgaard, W., Grootes, P., Hoffmann, G., Johnsen, S.  
2 J., Koster, R. D., Peel, D., Shuman, C. A., Stievenard, M., Stuiver, M., and White, J.: Validity  
3 of the temperature reconstruction from water isotopes in ice cores, *J. Geophys. Res. Oceans*,  
4 102, 26471-26487, 1997a.

5 Jouzel, J., Froehlich, K., and Schotterer, U.: Deuterium and oxygen-18 in present-day  
6 precipitation: data and modelling, *Hydrogeological science*, 42, 747-763, 1997b.

7 Jouzel, J. and Merlivat, L.: Deuterium and O-18 in precipitation- modelling of the isotopic  
8 effects during snow formation, *J. Geophys. Res.-Atmos.*, 89, 1749-1757, 1984.

9 Kaufmann, P., Federer, U., Hutterli, M. A., Bigler, M., Schüpbach, S., Ruth, U., Schmitt, J.,  
10 and Stocker, T. F.: An Improved Continuous Flow Analysis System for High-Resolution Field  
11 Measurements on Ice Cores, *Environ. Sci. Technol.*, 42, 8044-8050, doi: 10.1021/es8007722,  
12 2008.

13 Kinnard, C., Zdanowicz, C. M., Fisher, D. A., Isaksson, E., de Vernal, A., and Thompson, L.  
14 G.: Reconstructed changes in Arctic sea ice over the past 1,450 years, *Nature*, 479, 509-512,  
15 2011.

16 Koch, J. P. and Wegener, A.: *Wissenschaftliche Ergebnisse der dänischen Expedition nach*  
17 *Dronning Louises-Land und quer über das Inlandeis von Nordgrönland 1912-13*, Reitzel, 1930.

18 Lavigne, F., Degeai, J.-P., Komorowski, J.-C., Guillet, S., Robert, V., Lahitte, P., Oppenheimer,  
19 C., Stoffel, M., Vidal, C. M., Surono, Pratomo, I., Wassmer, P., Hajdas, I., Hadmoko, D. S.,  
20 and de Belizal, E.: Source of the great A.D. 1257 mystery eruption unveiled, Samalas volcano,  
21 Rinjani Volcanic Complex, Indonesia, *Proceedings of the National Academy of Sciences*, 110,  
22 16742-16747, 2013.

23 Mann, M. E., Bradley, R. S., and Hughes, M. K.: Global-scale temperature patterns and climate  
24 forcing over the past six centuries, *Nature*, 392, 779-787, 1998.

25 Mann, M. E., Zhang, Z., Rutherford, S., Bradley, R. S., Hughes, M. K., Shindell, D., Ammann,  
26 C., Faluvegi, G., and Ni, F.: Global Signatures and Dynamical Origins of the Little Ice Age and  
27 Medieval Climate Anomaly, *Science*, 326, 1256-1260, 2009.

28 Masson-Delmotte, V., Steen-Larsen, H. C., Ortega, P., Swingedouw, D., Popp, T., Vinther, B.  
29 M., Oerter, H., Sveinbjornsdottir, A. E., Gudlaugsdottir, H., Box, J. E., Falourd, S., Fettweis,  
30 X., Gallée, H., Garnier, E., Jouzel, J., Landais, A., Minster, B., Paradis, N., Orsi, A., Risi, C.,  
31 Werner, M., and White, J. W. C.: Recent changes in north-west Greenland climate documented

1 by NEEM shallow ice core data and simulations, and implications for past temperature  
2 reconstructions, *The Cryosphere*, 9, 1481-1504, 2015.

3 Merlivat, L. and Jouzel, J.: Global climatic interpretation of the deuterium-oxygen 18  
4 relationship for precipitation, *J. Geophys. Res.-Ocs. and Atmos.*, 84, 5029-5033, 1979.

5 Mieding, B.: Reconstruction of millennial aerosol-chemical ice core records from the northeast  
6 Greenland: Quantification of temporal changes in atmospheric circulation, emission and  
7 deposition, *Reports on Polar and Marine Reports*, 513, Alfred Wegener Institute for Polar and  
8 Marine Research, Bremerhaven, 2005.

9 Miller, G. H., Geirsdóttir, Á., Zhong, Y., Larsen, D. J., Otto-Bliesner, B. L., Holland, M. M.,  
10 Bailey, D. A., Refsnider, K. A., Lehman, S. J., Southon, J. R., Anderson, C., Björnsson, H., and  
11 Thordarson, T.: Abrupt onset of the Little Ice Age triggered by volcanism and sustained by sea-  
12 ice/ocean feedbacks, *Geophys. Res. Lett.*, 39, L02708, doi: 10.1029/2011GL050168, 2012.

13 Newhall, C. G. and Self, S.: The volcanic explosivity index (VEI) an estimate of explosive  
14 magnitude for historical volcanism, *J. Geophys. Res. Oceans*, 87, 1231-1238, 1982.

15 North Greenland Ice Core Project Members: Andersen, K. K., Azuma, N., Barnola, J.-M.,  
16 Bigler, M., Biscaye, P., Caillon, N., Chappellaz, J., Clausen, H. B., Dahl-Jensen, D., Fischer,  
17 H., Flückiger, J., Fritzsche, D., Fujii, Y., Goto-Azuma, K., Grønvold, K., Gundestrup, N. S.,  
18 Hansson, M., Huber, C., Hvidberg, C. S., Johnsen, S. J., Jonsell, U., Jouzel, J., Kipfstuhl, S.,  
19 Landais, A., Leuenberger, M., Lorrain, R., Masson-Delmotte, V., Miller, H., Motoyama, H.,  
20 Narita, H., Popp, T., Rasmussen, S. O., Raynaud, D., Rothlisberger, R., Ruth, U., Samyn, D.,  
21 Schwander, J., Shoji, H., Siggard-Andersen, M.-L., Steffensen, J. P., Stocker, T. F.,  
22 Sveinbjörnsdóttir, A. E., Svensson, A., Takata, M., Tison, J.-L., Thorsteinsson, T., Watanabe,  
23 O., Wilhelms, F., and White, J. W. C.: High-resolution record of Northern Hemisphere climate  
24 extending into the last interglacial period, *Nature*, 431, 147-151, 2004.

25 Ohmura, A.: New temperature distribution maps for Greenland, *Zeitschrift für Gletscherkunde  
26 und Glaziologie*, 35, 1-20, 1987.

27 Opel, T., Fritzsche, D., and Meyer, H.: Eurasian Arctic climate over the past millennium as  
28 recorded in the Akademii Nauk ice core (Severnaya Zemlya), *Clim. Past*, 9, 2379-2389, doi:  
29 10.5194/cp-9-2379-2013, 2013.

30 Ortega, P., Swingedouw, D., Masson-Delmotte, V., Risi, C., Vinther, B., Yiou, P., Vautard, R.,  
31 and Yoshimura, K.: Characterizing atmospheric circulation signals in Greenland ice cores:  
32 insights from a weather regime approach, *Clim. Dyn.*, 43, 2585-2605, 2014.

1 Pages2k, Consortium: Continental-scale temperature variability during the past two millennia,  
2 Nature Geosci., 6, 339-346, 2013.

3 Pinzer, B. R., Schneebeli, M., and Kaempfer, T. U.: Vapor flux and recrystallization during dry  
4 snow metamorphism under a steady temperature gradient as observed by time-lapse micro-  
5 tomography, The Cryosphere, 6, 1141-1155, doi: 10.5194/tc-6-1141-2012, 2012.

6 Robock, A.: Volcanic eruptions and climate, Rev. Geophys., 38, 191-219, 2000.

7 Schwager, M.: Ice core analysis on the spatial and temporal variability of temperature and  
8 precipitation during the late Holocene in North Greenland, Reports on Polar and Marine  
9 Research, 362, Alfred Wegener Institute for Polar and Marine Research, Bremen, 2000.

10 Semenov, V. A. and Latif, M.: The early twentieth century warming and winter Arctic sea ice,  
11 The Cryosphere, 6, 1231-1237, 2012.

12 Severinghaus, J. P., Sowers, T., Brook, E. J., Alley, R. B., and Bender, M. L.: Timing of abrupt  
13 climate change at the end of the Younger Dryas interval from thermally fractionated gases in  
14 polar ice, Nature, 391, 141-146, 1998.

15 Sigl, M., McConnell, J. R., Layman, L., Maselli, O., McGwire, K., Pasteris, D., Dahl-Jensen,  
16 D., Steffensen, J. P., Vinther, B., Edwards, R., Mulvaney, R., and Kipfstuhl, S.: A new bipolar  
17 ice core record of volcanism from WAIS Divide and NEEM and implications for climate  
18 forcing of the last 2000 years, J. Geophys. Res.-Atmos., 118, 1151-1169, 2013.

19 Sime, L. C., Risi, C., Tindall, J. C., Sjolte, J., Wolff, E. W., Masson-Delmotte, V., and Capron,  
20 E.: Warm climate isotopic simulations: what do we learn about interglacial signals in Greenland  
21 ice cores?, Quaternary. Sci. Rev., 67, 59-80, 2013.

22 Steen-Larsen, H. C., Masson-Delmotte, V., Hirabayashi, M., Winkler, R., Satow, K., Prié, F.,  
23 Bayou, N., Brun, E., Cuffey, K. M., Dahl-Jensen, D., Dumont, M., Guillevic, M., Kipfstuhl, S.,  
24 Landais, A., Popp, T., Risi, C., Steffen, K., Stenni, B., and Sveinbjörnsdóttir, A. E.: What  
25 controls the isotopic composition of Greenland surface snow?, Clim. Past, 10, 377-392, doi:  
26 10.5194/cp-10-377-2014, 2014.

27 Steen-Larsen, H. C., Masson-Delmotte, V., Sjolte, J., Johnsen, S. J., Vinther, B. M., Bréon, F.  
28 M., Clausen, H. B., Dahl-Jensen, D., Falourd, S., Fettweis, X., Gallée, H., Jouzel, J., Kageyama,  
29 M., Lerche, H., Minster, B., Picard, G., Punge, H. J., Risi, C., Salas, D., Schwander, J., Steffen,  
30 K., Sveinbjörnsdóttir, A. E., Svensson, A., and White, J.: Understanding the climatic signal in

1 the water stable isotope records from the NEEM shallow firn/ice cores in northwest Greenland,  
2 *J. Geophys. Res.-Atmos.*, 116, D06108, doi: 10.1029/2010JD014311, 2011.

3 Steffensen, J. P., Andersen, K. K., Bigler, M., Clausen, H. B., Dahl-Jensen, D., Fischer, H.,  
4 Goto-Azuma, K., Hansson, M., Johnsen, S. J., Jouzel, J., Masson-Delmotte, V., Popp, T.,  
5 Rasmussen, S. O., Rothlisberger, R., Ruth, U., Stauffer, B., Siggaard-Andersen, M. L.,  
6 Sveinbjornsdottir, A. E., Svensson, A., and White, J. W.: High-resolution Greenland ice core  
7 data show abrupt climate change happens in few years, *Science*, 321, 680-684, 2008.

8 Steinhilber, F., Beer, J., and Fröhlich, C.: Total solar irradiance during the Holocene, *Geophys.*  
9 *Res. Lett.*, 36, L19704, doi: 1029/2009GL040142, 2009.

10 Vinther, B. M., Andersen, K. K., Hansen, A. W., Schmith, T., and Jones, P. D.: Improving the  
11 Gibraltar/Reykjavik NAO index, *Geophys. Res. Lett.*, 30, 2222, doi: 10.1029/2003GL018220,  
12 2003.

13 Vinther, B. M., Andersen, K. K., Jones, P. D., Briffa, K. R., and Cappelen, J.: Extending  
14 Greenland temperature records into the late eighteenth century, *J. Geophys. Res.-Atmos.*, 111,  
15 D11105, doi: 10.1029/2005JD006810, 2006a.

16 Vinther, B. M., Buchardt, S. L., Clausen, H. B., Dahl-Jensen, D., Johnsen, S. J., Fisher, D. A.,  
17 Koerner, R. M., Raynaud, D., Lipenkov, V., Andersen, K. K., Blunier, T., Rasmussen, S. O.,  
18 Steffensen, J. P., and Svensson, A. M.: Holocene thinning of the Greenland ice sheet, *Nature*,  
19 461, 385-388, 2009.

20 Vinther, B. M., Clausen, H. B., Fisher, D. A., Koerner, R. M., Johnsen, S. J., Andersen, K. K.,  
21 Dahl-Jensen, D., Rasmussen, S. O., Steffensen, J. P., and Svensson, A. M.: Synchronizing ice  
22 cores from the Renland and Agassiz ice caps to the Greenland Ice Core Chronology, *J.*  
23 *Geophys. Res.-Atmos.*, 113, D08115, doi: 10.1029/2007JD009143, 2008.

24 Vinther, B. M., Clausen, H. B., Johnsen, S. J., Rasmussen, S. O., Andersen, K. K., Buchardt, S.  
25 L., Dahl-Jensen, D., Seierstad, I. K., Siggaard-Andersen, M. L., Steffensen, J. P., Svensson, A.,  
26 Olsen, J., and Heinemeier, J.: A synchronized dating of three Greenland ice cores throughout  
27 the Holocene, *J. Geophys. Res.-Atmos.*, 111, D13102, doi: 10.1029/2005JD006921, 2006b.

28 Vinther, B. M., Jones, P. D., Briffa, K. R., Clausen, H. B., Andersen, K. K., Dahl-Jensen, D.,  
29 and Johnsen, S. J.: Climatic signals in multiple highly resolved stable isotope records from  
30 Greenland, *Quat. Sci. Rev.*, 29, 522-538, 2010.

31 Weißbach, S., Wegener, A., and Kipfstuhl, J.: Snow accumulation in North Greenland over the  
32 last millennium. In: *Towards an interdisciplinary approach in earth system science*, edited by:

- 1 Lohmann, G., Meggers, H., Unnithan, V., Wolf-Gladrow, D., Notholt, J., and Bracher, A.,  
2 Springer Earth System Science, London, 197-205, 2015.
- 3 Werner, M.: Vergleichende Studie ueber die Verteilung vulkanogener Spurenstoffdepositionen  
4 in Nord-Ost-Groenland, Diplom, Institut fuer Umweltphysik, Heidelberg, 85 pp., 1995.
- 5 White, J. W. C., Barlow, L. K., Fisher, D., Grootes, P., Jouzel, J., Johnsen, S. J., Stuiver, M.,  
6 and Clausen, H.: The climate signal in the stable isotopes of snow from Summit, Greenland:  
7 Results of comparisons with modern climate observations, *J. Geophys. Res. Oceans*, 102,  
8 26425-26439, 1997.
- 9 Wilhelms, F.: Leitfähigkeits- und Dichtemessung an Eisbohrkernen, Reports on Polar and  
10 Marine Research, 191, Alfred Wegener Institute for Polar and Marine Research, Bremerhaven,  
11 1996.
- 12 Wood, K. R. and Overland, J. E.: Early 20th century Arctic warming in retrospect, *Int. J.*  
13 *Climatol.*, 30, 1269-1279, 2010.
- 14 Wood, K. R., Overland, J. E., Jónsson, T., and Smoliak, B. V.: Air temperature variations on  
15 the Atlantic-Arctic boundary since 1802, *Geophys. Res. Lett.*, 37, L17708, doi:  
16 10.1029/2010GL044176, 2010.
- 17 Zielinski, G. A.: Use of paleo-records in determining variability within the volcanism–climate  
18 system, *Quat. Sci. Rev.*, 19, 417-438, 2000.

1 Table 1. Overview of all NGT drill sites.

Core Id	Core length (m)	Elevation (m a. sl.)	Geographic Position	
			Latitude (°N)	Longitude (°W)
B16	102.4	3040	73.94	37.63
B17	100.8	2820	75.25	37.63
B18	150.2	2508	76.62	36.40
B19	150.4	2234	78.00	36.40
B20	150.4	2147	78.83	36.50
B21	100.6	2185	80.00	41.14
B22	120.6	2242	79.34	45.91
B23	150.8	2543	78.00	44.00
B26	119.7	2598	77.25	49.22
B27	175.0	2733	76.66	46.82
B28	70.7	2733	76.66	46.82
B29	110.5	2874	76.00	43.50
B30	160.8	2947	75.00	42.00

2

Table 2. Depth of volcanic horizons used for dating. The given year is the time of aerosol deposition on the Greenlandic Ice Sheet. All depths are given in meter water equivalent. If a horizon could not be clearly identified a hyphen is shown in the table. A field is empty if the horizon is deeper than the length of the ice core. The maximum difference is estimated from a comparison between cores dated by annual layer counting (Mieding, 2005; Schwager, 2000) and the dating used for this study. Given is also the VEI (Newhall and Self, 1982) and the total northern hemisphere stratospheric sulfate aerosol injection (Gao et al., 2008) for each used volcanic eruption.

\*)(*Sigl et al., 2013*), \*\*)(*Friedmann et al., 1995*)

Year [AD]	Event	B16	B17	B18	B19	B20	B21	B22	B23	B26	B27	B28	B29	B30	VEI	Sulfate
<b>1912</b>	Katmai*	11.60	9.31	8.48	7.38	7.86	8.62	11.56	9.49	14.27	13.69	14.44	11.41	13.12	6	11.0
<b>1816</b>	Tambora*	24.49	20.27	18.91	16.77	17.27	19.46	26.17	21.54	31.50	31.13	31.91	25.97	29.91	7	58.7
<b>1783</b>	Laki*	29.36	24.19	22.45	19.94	20.32	23.10	31.25	25.93	37.77	37.19	38.07	31.28	35.80	4	93.0
<b>1739</b>	Tarumai*	35.52	-	26.90	24.10	24.62	-	-	-	-	-	-	-	43.07	5	0
<b>1694</b>	Hekla**	-	34.47	31.84	28.54	29.16	32.87	44.06	-	-	-	-	44.22	50.45	4	0
<b>1666</b>	Unknown**	46.22	-	34.75	31.20	32.10	35.93	48.13	-	-	-	-	48.50	-		0
<b>1640</b>	Komagatake**	49.90	-	37.48	33.69	34.80	-	-	-	-	-	-	52.36	-	4	33.8
<b>1601</b>	Huaynaputina*		44.97	41.62	-	38.70	42.95	-	48.31	69.22	68.39		58.25	65.94	4	46.1
<b>1479</b>	Mt. St. Helenes**		58.84	54.42	-	51.31	56.04	75.09	-		89.42		76.81	86.60		7.4
<b>1259</b>	Samalas*			76.60	68.03	72.86			89.35		126.10			122.10		145.8
<b>1179</b>	Katla*			-	-	80.04			98.60							0
<b>934</b>	Eldgia*			109.20	99.20											0
Max. age of core [AD]		1470	1363	874	753	775	1372	1372	1023	1505	1195	1763	1471	1242		
Max. difference [a]		7		3		8	6			4			3			

1 Table 3. Resulting mean accumulation rates (from the surface to the deepest volcanic horizon  
 2 and in brackets for their common time window (1505-1953 AD)) for each NGT drill site, the  
 3 lowest and highest rate within the whole core length, the time period from surface to the  
 4 deepest volcanic horizon and the age at the bottom of the ice core calculated by extrapolation  
 5 of the deepest calculated accumulation rate.

Core	Mean accumulation rate [kg m <sup>-2</sup> a <sup>-1</sup> ]	Accumulation rate range [kg m <sup>-2</sup> a <sup>-1</sup> ]	Time period [AD]	Age at bottom of core[AD]
B16	141 [141]	134-148	1640-1993	1470
B17	114 [114]	113-119	1479-1993	1363
B18	103 [106]	100-110	934-1993	874
B19	94 [94]	90-99	934-1993	753
B20	98 [100]	90-105	1179-1994	775
B21	109 [109]	105-113	1479-1994	1372
B22	145 [145]	141-154	1479-1994	1372
B23	121 [122]	116-132	1179-1994	1023
B26	176 [176]	172-190	1601-1995	1505
B27/B28	180 [181]	165-187	1783-1995	1195
B29	149 [150]	137-161	1479-1995	1471
B30	166 [169]	158-178	1259-1995	1242

6



1 Table 4. The 15-m firn temperature, mean annual  $\delta^{18}\text{O}$  values for each ice core, the range of  
 2 the highest and lowest  $\delta^{18}\text{O}$  values and the year they occurred as well as the standard deviation  
 3 (SD) all given for their common time window (1953-1505 AD).

4 \*(*Vinther et al., 2006b*), \*\*(*Schwager, 2000*), \*\*\* *interpolated from (Schwager, 2000)*

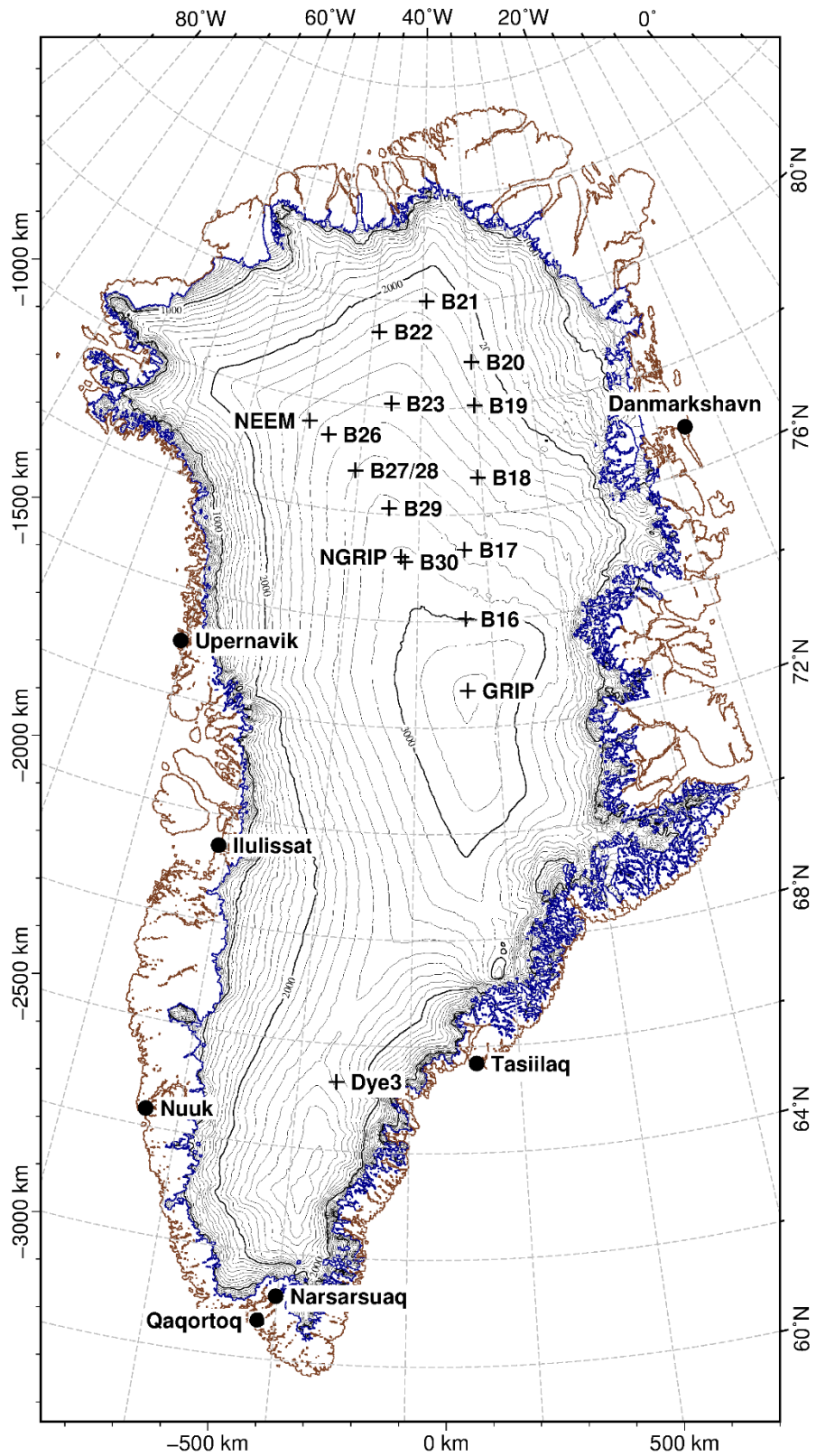
Core	15 m Firn temperature [°C]	Mean $\delta^{18}\text{O}$ [‰]	$\delta^{18}\text{O}$ range [‰]	Years [AD] of lowest- highest value	SD $\delta^{18}\text{O}$ [‰]	Time period [AD] (whole core length)
B16	-32.5***	-37.07	-40.64 to -33.11	1839-1937	0.99	1470-1993
B17	-32.3***	-37.13	-40.06 to -33.89	1835-1879	1.08	1363-1993
B18	-32.3***	-36.53	-41.52 to -31.75	1761-1889	1.44	874-1993
B19	-30.9 ( $\pm 0.5$ )**	-35.49	-38.97 to -31.77	1575-1826	1.32	753-1953
B20	-30.4***	-35.41	-39.34 to -30.69	1699-1929	1.42	775-1994
B21	-30.1***	-34.53	-38.29 to -30.95	1814-1871	1.29	1372-1994
B22	-29.8***	-34.54	-39.11 to -29.84	1921-1953	1.34	1372-1994
B23	-29.3 ( $\pm 0.5$ )**	-35.98	-42.11 to -32.23	1918-1928	1.28	1023-1994
B26	-30.3***	-33.86	-37.22 to -29.42	1597-1893	1.25	1505-1995
B27/B28	-30.6 ( $\pm 0.5$ )**	-34.47	-38.26 to -30.58	1566-1892	1.25	1195-1995
B29	-31.6 ( $\pm 0.5$ )**	-35.65	-39.22 to -31.59	1834-1928	1.18	1471-1995
B30	-31.8 ( $\pm 0.5$ )**	-35.46	-38.53 to -31.52	1862-1928	1.09	1242-1988
NGRIP*		-35.42	-40.12 to -30.81	1836-1928	1.24	

5

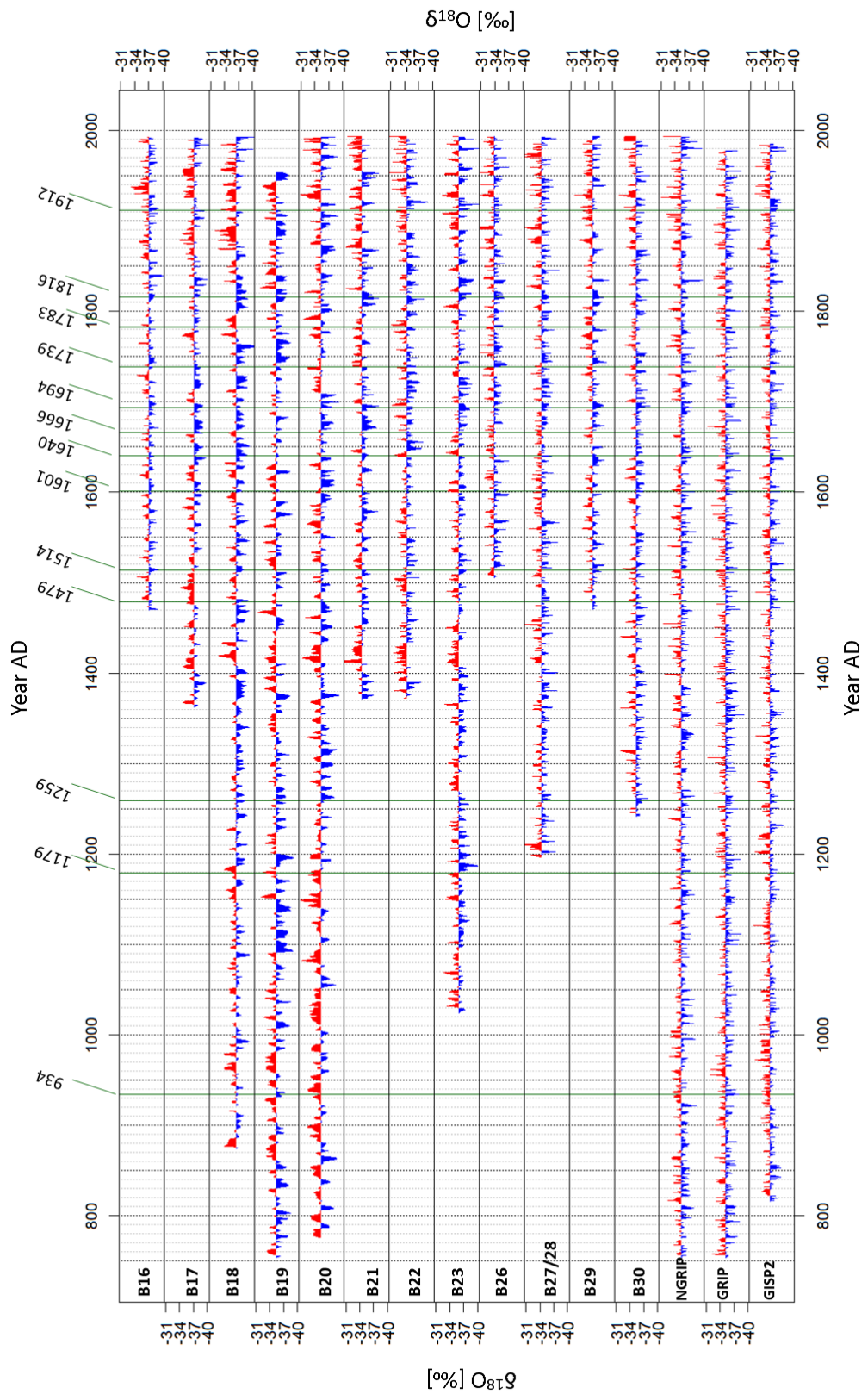
1 Table 5. Correlation coefficients (r) of the stacked  $\delta^{18}\text{O}$ -record with annual and seasonal (DJF,  
 2 MAM, JJA and SON) extended Greenland temperature records <sup>\*)</sup>(Vinther et al., 2006a), North  
 3 west Iceland instrumental data <sup>\*\*)</sup>(Hanna et al., 2004; Jónsson, 1989), annual mean Greenland  
 4 ice sheet near-surface air temperatures from combined instrumental and model output <sup>\*\*\*)</sup> (Box  
 5 et al., 2009) and Arctic temperature reconstruction <sup>\*\*\*\*)</sup>(Wood et al., 2010). All correlations are  
 6 done with 5-year running means and are significant on 95 % level ( $p < 0.05$ ).

	r	r	Years of overlap
	annual	seasonal	
*) Merged South (Greenland)	0.51	DJF	0.47
		MAM	0.62
		JJA	0.51
		SON	0.5
*) Ilulissat (Greenland)	0.46	DJF	0.50
		MAM	0.42
		JJA	0.36
		SON	0.45
*) Nuuk (Greenland)	0.41	DJF	-
		MAM	0.55
		JJA	0.47
		SON	0.47
*) Qaqortoq (Greenland)	0.39	DJF	-
		MAM	0.50
		JJA	0.50
		SON	0.36
**) Stykkisholmur (Iceland)	0.41	DJF	-
		MAM	0.36
		JJA	0.35
		SON	0.31
***) Mean Greenland surface air temperature	0.50		1840-1994
****) Extended instrumental temperature record	0.55		1802-1994

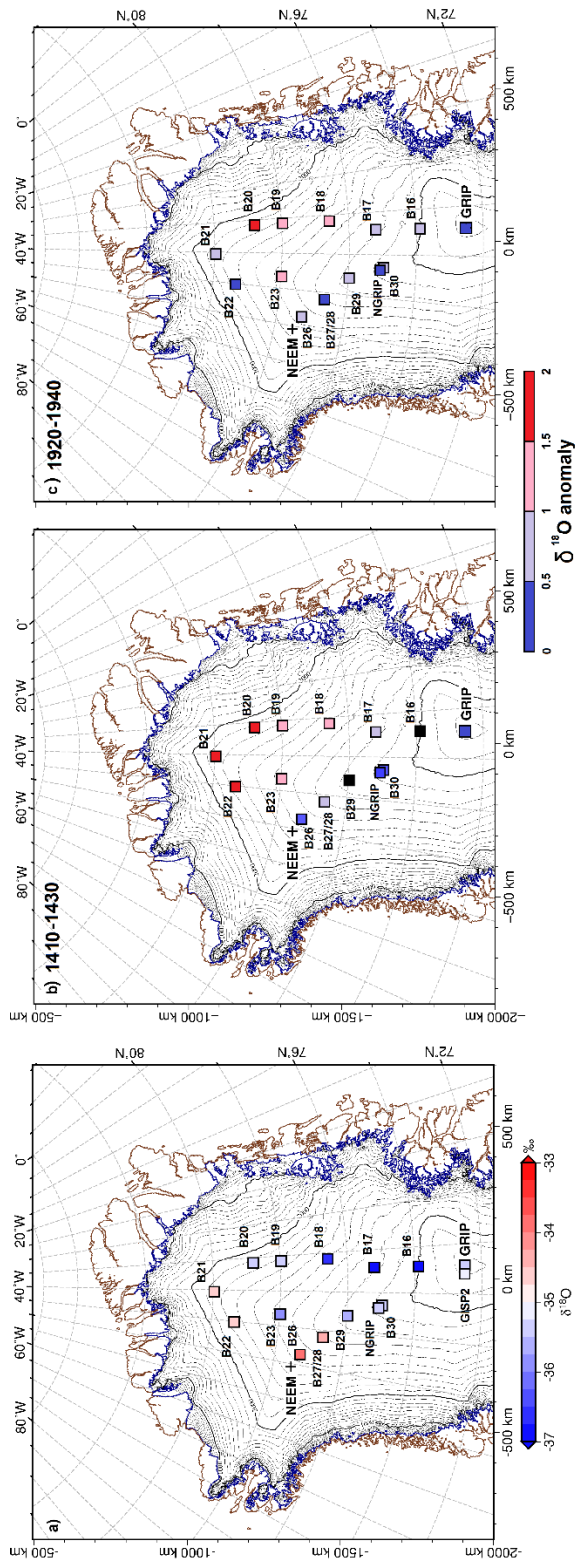
7



1  
 2 Figure 1. Map of Greenland with NGT ice cores (B16-B23, B26-B30 crosses), deep drilling  
 3 sites (crosses) and towns (black dots). The ice surface topography is according to Bamber et al.  
 4 (2013), (mapping: Polar Stereographic (WGS84), Standard Parallel 71, Latitude of Projection  
 5 Origin -39).

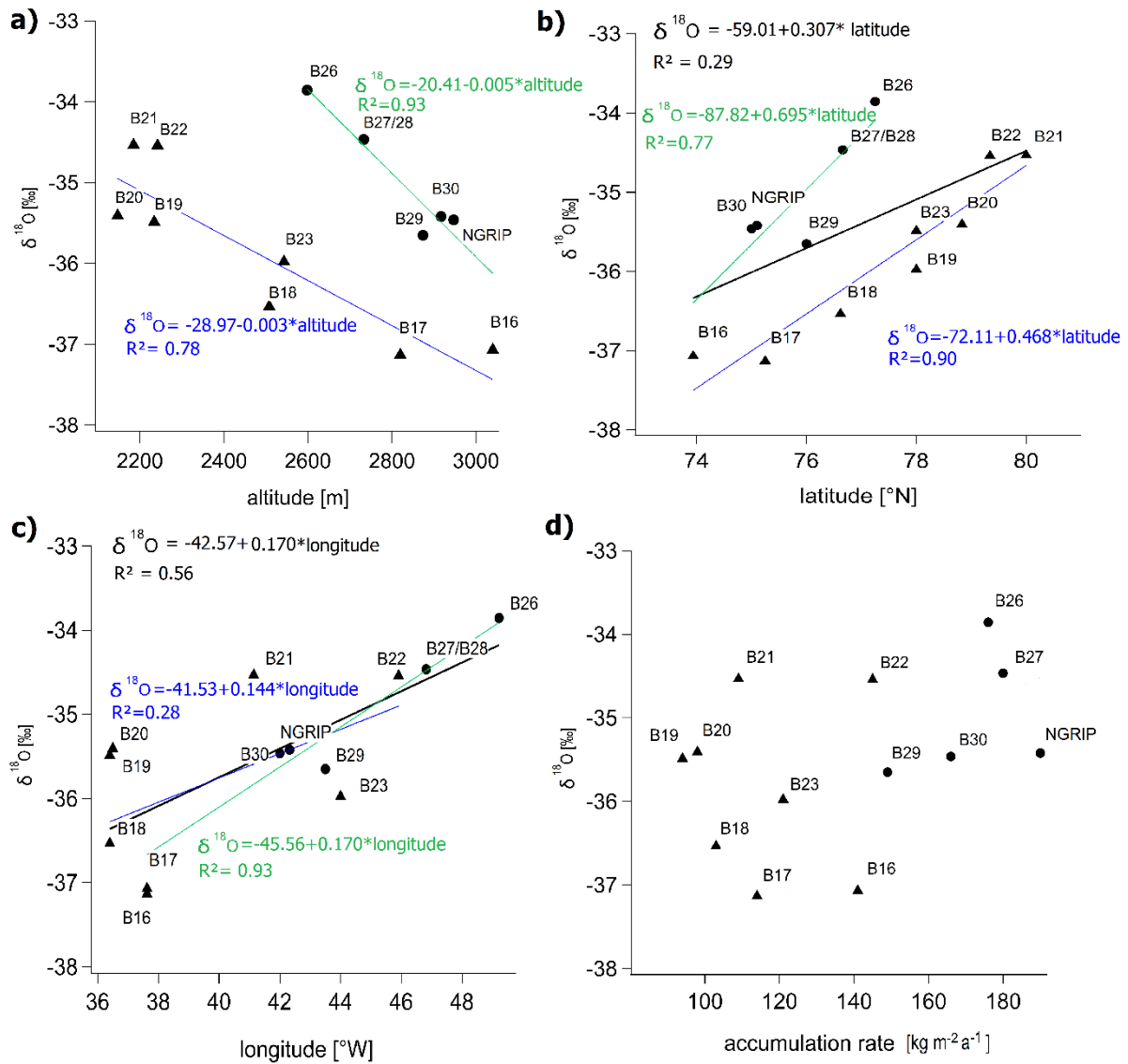


1  
 2 Figure 2. Annual  $\delta^{18}\text{O}$  records at the 12 NGT sites (this study) and NGRIP (Vinther et al.,  
 3 2006b), GRIP (Vinther et al., 2010) and GISP2 (Grootes and Stuiver, 1997). Blue are the values  
 4 below the mean over their common time window (1505 -1953 AD) and red are the higher ones.  
 5 Dark green vertical lines mark the volcanic eruptions (years given at top) used as time markers.



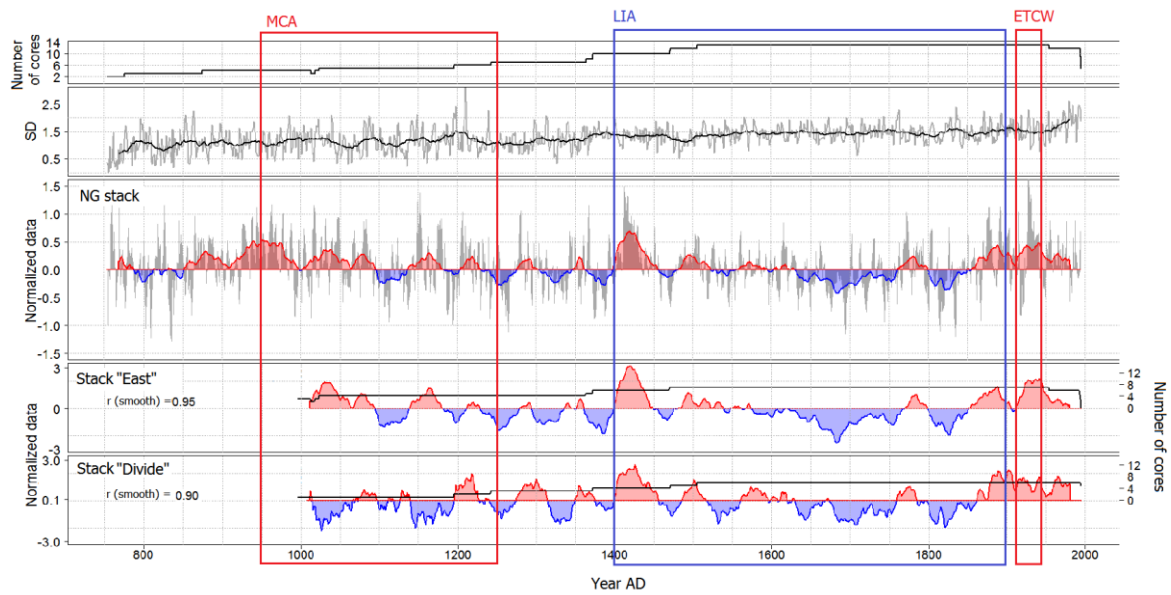
1  
 2 Figure 3. Spatial distribution of  $\delta^{18}\text{O}$  values in northern Greenland. a) The mean  $\delta^{18}\text{O}$  values of  
 3 the northern Greenland ice cores in their common time window (1505-1953 AD) is given with  
 4 color coded squares. Blue colors representing lighter values, red colors heavier values.  
 5 Mapped mean anomalies of  $\delta^{18}\text{O}$  compared to a) for two different periods: b) 1410-1430 AD  
 6 and c) 1920-1940 AD. If a record not cover the required time period the square is filled in black.

1



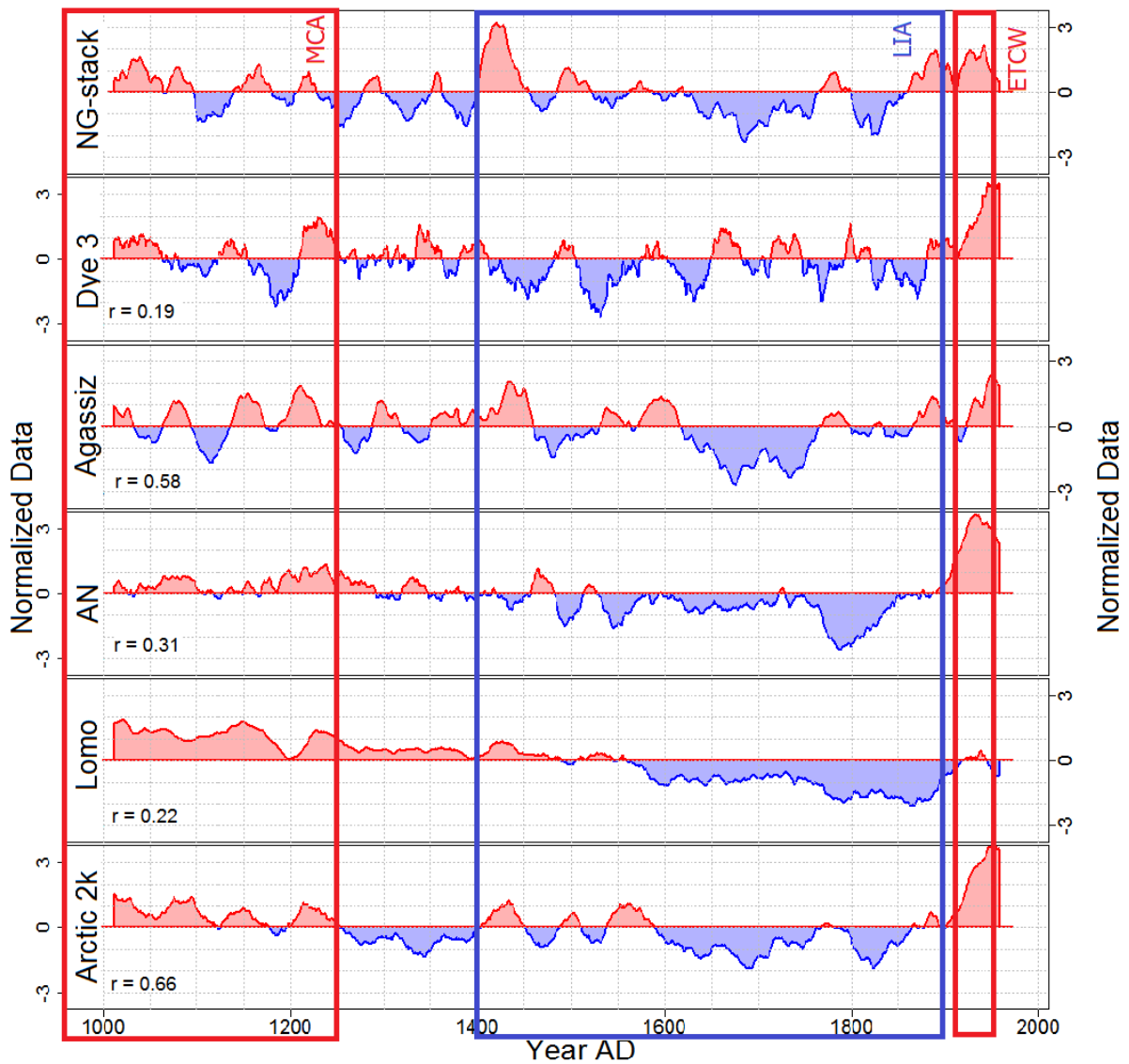
2

3 Figure 4. Mean  $\delta^{18}\text{O}$  (1505-1953 AD) as a function of a) altitude, b) latitude and c) longitude  
 4 d) accumulation rate of northern Greenland ice core drill sites. Cores with higher accumulation  
 5 rates ( $<145 \text{ kg m}^{-2} \text{ a}^{-1}$ ) are given as black dots and lower rates as black triangles, which is similar  
 6 to the differentiation between east of and on the main ice divide. For statistically significant  
 7 correlations the lines give the linear regression functions (black: mean, green: higher  
 8 accumulation rates, blue: lower accumulation rates).



1  
2 Figure 5. At top of the figure the number of cores used for the stack and the standard deviation  
3 (SD, gray: annual values, black: 30-year running mean) of all times are given.  
4 Middle: Annual stacked  $\delta^{18}\text{O}$  (grey) and smoothed record (30-year running mean). Values more  
5 enriched compared to the mean (1953-1505 AD) are red, values less enriched are shown in  
6 blue. Known climate anomalies are marked: Medieval Climate Anomaly (MCA, 950 - 1250  
7 AD (Mann et al., 2009)), the Little Ice Age (LIA, 1400 - 1900 AD (Mann et al., 1998)), Early  
8 Twentieth Century Warming (ETCW, 1920 – 1940 (Semenov and Latif, 2012; Wood and  
9 Overland, 2010)).  
10 Bottom: 30-year running mean on z-levels (centred and normalized data) of stacked northern  
11 Greenland  $\delta^{18}\text{O}$  records over the last 1000 years. Stack “East”: B16, B17, B18, B19, B20, B21  
12 and B23, stack “Divide”: B22, B26, B27, B29, B30 and NGRIP. Values in red are more  
13 enriched compared to the mean over their last 1000 years, and blue are less enriched. Given is  
14 also the correlation coefficient of 30- year running means between the NG-stack and the sub-  
15 stacks (1505-1993 AD). The coefficient for a similar correlation between the two substacks is  
16 calculated with  $r = 0.71$ .

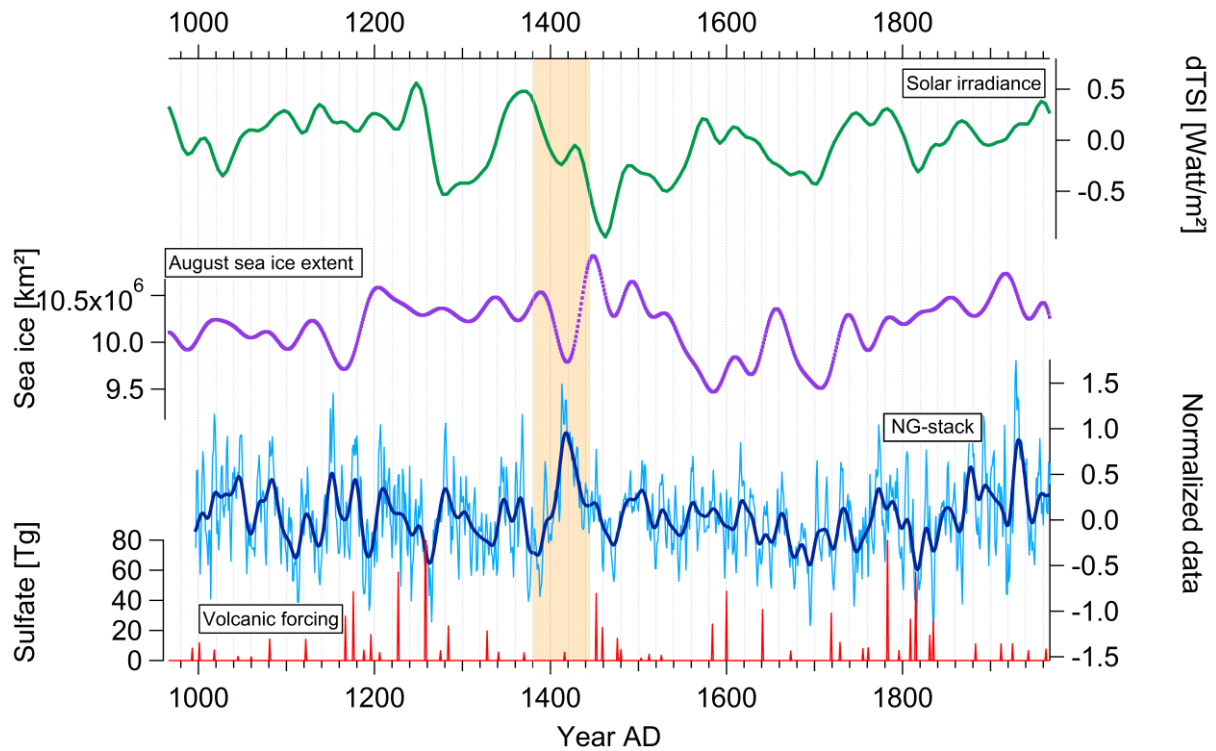
1



2

3 Figure 6. 30-year running mean for  $\delta^{18}\text{O}$ -values from different Arctic regions: northern  
4 Greenland (NG-stack, this study), southern Greenland (Dye3, Vinther et al., 2006b),  
5 Canada (Agassiz Ice Cap, Agassiz, Vinther et al., 2008), Russian Arctic (Akademii Nauk, AN,  
6 Opel et al., 2013), Svalbard (Lomonosofvonna, Lomo, Divine et al., 2011) and a  
7 reconstructed record (Arctic2k, Consortium Pages2k, 2013). All records are given on z-  
8 level scales (centered and normalized data). Also the correlation coefficient for the  
9 smoothed values to our stack is given.





1  
 2 Figure 7. The northern Greenland stack (NG-stack, blue: annual, dark blue: smoothed) is shown  
 3 with possible forcing factors: Green the reconstructed total solar irradiance (Steinhilber et al.,  
 4 2009), in purple the reconstructed August arctic sea- ice extent (Kinnard et al., 2011) and in  
 5 red at the bottom the stratospheric sulphate aerosol injection for the northern hemisphere (Gao  
 6 et al., 2008). All values are 40-year- low-pass filtered. The discussed 1420 AD event is marked  
 7 with beige colour.